

Quivers, YBE and 3-manifolds

Masahito Yamazaki

Princeton Center for Theoretical Science,
Princeton University, Princeton, NJ 08544, USA

Abstract

We study 4d superconformal indices for a large class of $\mathcal{N} = 1$ superconformal quiver gauge theories realized combinatorially as a bipartite graph or a set of “zig-zag paths” on a two-dimensional torus T^2 . An exchange of loops, which we call a “double Yang-Baxter move”, gives the Seiberg duality of the gauge theory, and the invariance of the index under the duality is translated into the Yang-Baxter-type equation of a spin system defined on a “Z-invariant” lattice on T^2 . When we compactify the gauge theory to 3d, Higgs the theory and then compactify further to 2d, the superconformal index reduces to an integral of quantum/classical dilogarithm functions. The saddle point of this integral unexpectedly reproduces the hyperbolic volume of a hyperbolic 3-manifold. The 3-manifold is obtained by gluing hyperbolic ideal polyhedra in \mathbb{H}^3 , each of which could be thought of as a 3d lift of the faces of the 2d bipartite graph. The same quantity is also related with the thermodynamic limit of the BPS partition function, or equivalently the genus 0 topological string partition function, on a toric Calabi-Yau manifold dual to quiver gauge theories. We also comment on brane realization of our theories. This paper is a companion to another paper summarizing the results [1].

1 Introduction and Summary

Four-dimensional supersymmetric quiver gauge theories has been a useful playground to understand the physics of strongly coupled phenomena of gauge theories, in particular their IR fixed points.

In this paper, we study a large class of 4d $\mathcal{N} = 1$ quiver gauge theories described combinatorially by a configuration of oriented cycles (called *zig-zag paths*) on a two-dimensional torus, satisfying certain conditions analyzed below [2]. This combinatorial data, equivalently expressed as a bipartite graph (dimer) or a quiver diagram on T^2 , encodes the matter content (the quiver diagram) and the Lagrangian of our gauge theories [3, 4, 5]. We here take the gauge group at each vertex of the quiver diagram to be $U(N)$. The resulting gauge theory is believed to flow to a non-trivial interacting fixed point in the IR, can be engineered from a stack of N D3-branes probing the tip of the a toric Calabi-Yau manifold, and has been extensively studied in the context of AdS/CFT correspondence (see [6, 7] and references therein).

There is an interesting subtlety in this story. The gauge theory corresponding to a given toric Calabi-Yau manifold is not unique, and several different gauge theories, related by a sequence of Seiberg dualities [8], correspond to the same geometry (this is sometimes called “toric duality”). In the language of zig-zag paths, this is translated into an ambiguity of the relative position of the loops, and Seiberg duality is translated into an exchange of the loops, which we call a “double Yang-Baxter move”. As the naming suggests, this is the standard Yang-Baxter move repeated twice, and strongly suggest the integrable structure behind the theory.

Given a 4d supersymmetric gauge theory, we could extract concrete quantitative statements of the theory by computing its 4d superconformal index I [9, 10]. This is a twisted partition function on $S^3 \times S^1$, where the chemical potentials are turned on along the S^1 direction. The index can be computed in the free field limit, and is written as a matrix integral. One of the main results of this paper is that this matrix model could be regarded as the partition function of a spin system defined from zig-zag paths on T^2 , where each spin has $N - 1$ continuous values in S^1 . This is summarized in the relation

$$I_{\text{4d quiver}} = Z_{\text{spin system on } T^2} . \tag{1.1}$$

This is the manifestation of the integrable structure mentioned above; the Seiberg duality is now translated into the statement that the resulting partition function is invariant under the double Yang-Baxter move, ensuring the integrability of the model. Interestingly, (modulo some important differences mentioned below) the resulting spin system is

essentially the same as the spin system studied in [11] for $SU(2)$ gauge groups, and more recently in [12] for $SU(N)$ gauge groups.

Let us next study the reduction of our 4d $\mathcal{N} = 1$ theories along S^1 . The resulting theory has 3d $\mathcal{N} = 2$ supersymmetry, and flows in the IRg to a non-trivial fixed point. As the S^1 shrinks all the KK modes decouple, and the 4d superconformal index should reduce to a partition function on S^3 . Indeed, it has been shown that the 4d index in this limit reduces (after suitably regularizing divergences) to a 3d partition function on ellipsoid S_b^3 (defined in (4.1)), which could be again written as a matrix integral after localization computation:

$$I_{4\text{d quiver}} \longrightarrow Z_{3\text{d on } S_b^3} . \quad (1.2)$$

This limit is also natural in the context of integrable models; the Yang-Baxter equation, being an equality, should hold even after taking the limit¹. After taking one more limit explained in the text (Higgsing to the Abelian gauge group), the solution of the star-triangle relation studied in [11] reduces to another solution discovered by Faddeev and Volkov [13, 14, 15], clarifying the integrable structure behind 3d $\mathcal{N} = 2$ theories.

We could also consider further dimensional reduction to 2d. This is simply the $b \rightarrow 0$ limit of the ellipsoid partition function, and taking the leading contribution we have

$$Z_{3\text{d on } S_b^3} \longrightarrow Z_{2\text{d on } \mathbb{R}^2} = \int d\sigma \exp \left[\frac{1}{2\pi b^2} \mathcal{W}_{2\text{d}}(\sigma) + \mathcal{O}(b^0) \right] , \quad (1.3)$$

where σ is the scalar component(s) of the twisted superfield (defined from the derivative of the vector superfield) and takes values in the Cartan of the gauge group². The potential $\mathcal{W}_{2\text{d}}(\sigma)$ represents the effective twisted superpotential obtained by integrating out matters from the theory.

The surprising observation, based on the works [16, 17], is that this twisted effective superpotential is identified with the hyperbolic volume of a certain 3-manifold M , in the case that $N = 2$.

The 3-manifold M is determined from the bipartite graph on T^2 which in turn is determined from zig-zag paths, and could be thought of as a 2d graph with an “extra dimension” added. The 3-manifold M is defined as the union of ideal hyperbolic polyhedra in \mathbb{H}^3 , and the projection of the polyhedra onto the boundary of \mathbb{H}^3 gives the faces of the 2d bipartite graph.

¹As we will see there are some subtleties associated with the regularization of divergences in the limit.

²In general σ is a vector, but we here do not show this fact explicitly for notational simplicity.

The twisted superfield scalars σ , in this description, is identified with the geometric modulus of the 3-manifold M ; the dihedral angles of M are determined from the radii of circles on T^2 , whose logarithms coincide with σ . The values of σ are determined from the gluing conditions of the 3-manifold M

$$\exp\left(\frac{\partial\text{Vol}[M](\sigma)}{\partial\sigma}\right) = 1 . \quad (1.4)$$

There is a counterpart of this equation on the gauge theory side; the value of σ at the vacuum is determined from the equation

$$\exp\left(\frac{\partial\mathcal{W}_{2d}}{\partial\sigma}\right) = 1 . \quad (1.5)$$

We find that the two conditions (1.4), (1.5) coincide. In other words, the vacua of the 2d $\mathcal{N} = (2, 2)$ theory is captured by the gluing condition of the 3-manifold! This is the second main result of our paper.

One quick supporting evidence for the correspondence between (1.4) and (1.5) is that the twisted superpotential \mathcal{W}_{2d} is expressed as a sum of the Lobachevsky functions (or classical dilogarithm functions), and the same function is known to appear in the formula for the volume of hyperbolic tetrahedra; M is simply the sum of these tetrahedra. Of course, the appearance of the dilogarithm function applies to any 3d $\mathcal{N} = 2$ theories dimensionally reduced on S^1 , whereas our correspondence should hold only for a specific class of 3d gauge theories.

In Table 1 we summarize our correspondence between 2d $\mathcal{N} = (2, 2)$ theory and the geometry of the 3-manifold M . The data on both sides come from the zig-zag paths on T^2 , and therefore from a toric Calabi-Yau 3-fold or from the brane configuration for our gauge theories.

Table 1: Dictionary between the 2d $\mathcal{N} = (2, 2)$ theories and the 3-manifold.

2d $\mathcal{N} = (2, 2)$ gauge theory	3-manifold
twisted superpotential $\mathcal{W}_{2d}(\sigma)$	$\text{Vol}[M](\sigma)$
scalar in twisted superfield σ	modulus σ of M
matter contributing Li_2	tetrahedron contributing Li_2
vacuum equation $\exp\left(\frac{\partial\mathcal{W}}{\partial\sigma}\right) = 1$	gluing condition $\exp\left(\frac{\partial M}{\partial\sigma}\right) = 1$

The correspondence to this point refers only to the 2d gauge theory. However, it is natural to ask if similar correspondence persists for the 3d/4d gauge theories we started

with. As for the 3d gauge theory, the natural guess is to propose

$$Z_{3\text{d on } S_b^3} \sim Z_{3\text{d } SL(2) \text{ Chern-Simons on } M} , \quad (1.6)$$

where the right hand side is the (holomorphic) partition function of the $SL(2)$ Chern-Simons theory on M and the parameter b is identified with the inverse square root of the level t of the Chern-Simons theory: $b^2 \sim 1/(t+2)$. This is consistent with our previous correspondence since the classical limit of the $SL(2)$ Chern-Simons theory reproduces the volume (and the Chern-Simons invariant) of the 3-manifold. There is also generalization of (1.6) to $N > 2$, where the right hand is replaced by the partition function of $SL(N)$ Chern-Simons theory on M .

The relation (1.6), relating 3d $\mathcal{N} = 2$ quiver gauge theories and the 3d $SL(2)$ Chern-Simons theory, is highly reminiscent of the recently found connection [18, 19, 20, 21, 22, 23, 24] between 3d $\mathcal{N} = 2$ theories and 3d $SL(2)$ Chern-Simons theories (see also [25]). There one of the crucial underlying data is the Riemann surface and its Teichmüller space, whereas here we have a dimer as the crucial ingredient. We expect that this similarity could be explained from the equivalence of underlying mathematical structures (for example, cluster algebras), perhaps along the lines of [26] (*cf.* [27, 23, 28]). It would be interesting to understand the precise relation between the two.

Let us also comment on the relation between (1.1) and (1.6). It is natural to interpret both statements from compactification of a 6d theory (see the discussion in section 2.3 and 4.5). If this is true, then the two statements are related by a dimensional reduction on the one hand, and by a dimensional oxidation on the other side, thus exemplifying the statement (*cf.* [29, section 5])

$$\text{dimensional reduction} = \text{dimensional oxidation}$$

in the AGT[30]-type correspondence.

Finally, we point out connection of our results to topological string theory and the BPS state counting.

Under an assumption about the bipartite graph (isoradiality condition in section 2.2), we show that the critical value of the hyperbolic volume of our 3-manifold M could be written as a sum of Lobachevsky functions (see (4.38)). Interestingly, exactly the same expression arises as a Legendre transform of the thermodynamic limit of the partition function of the dimer model. This dimer model has been studied in the context of BPS state counting of type IIA string theory on a Calabi-Yau 3-manifold X_Δ , which in turn is

known to be equivalent to the topological string partition function (modulo wall crossing phenomena). In this context the thermodynamic limit is the semiclassical limit $g_{\text{top}} \rightarrow 0$, where g_{top} is the topological string coupling constant, and the leading contribution is precisely the prepotential $\mathcal{F}_{\text{top},0}$ [31]. Combining these observations, we have

$$\mathcal{F}_{\text{top},0} \text{ is an integral of the Legendre transformation of } \text{Vol}[M_0] . \quad (1.7)$$

This paper is companion to [1], which announces basic results.

This paper is organized as follows (see Figure 1 for the logical structure of this paper). After a summary of 4d $\mathcal{N} = 1$ quiver gauge theories described from zig-zag paths (section 2), we compute its superconformal index and comment on the reformulation as a spin system (section 3). We then reduce the theory down to 3d and 2d, and study the connection with 3-manifolds (section 4). Section 5 explains the relation with topological string theory and the statistical mechanical model of BPS state melting. We conclude with some future problems (section 6). Appendix contains a summary of the special functions used in the main text, and an explicit computation of thermodynamic limit of the dimer partition function.

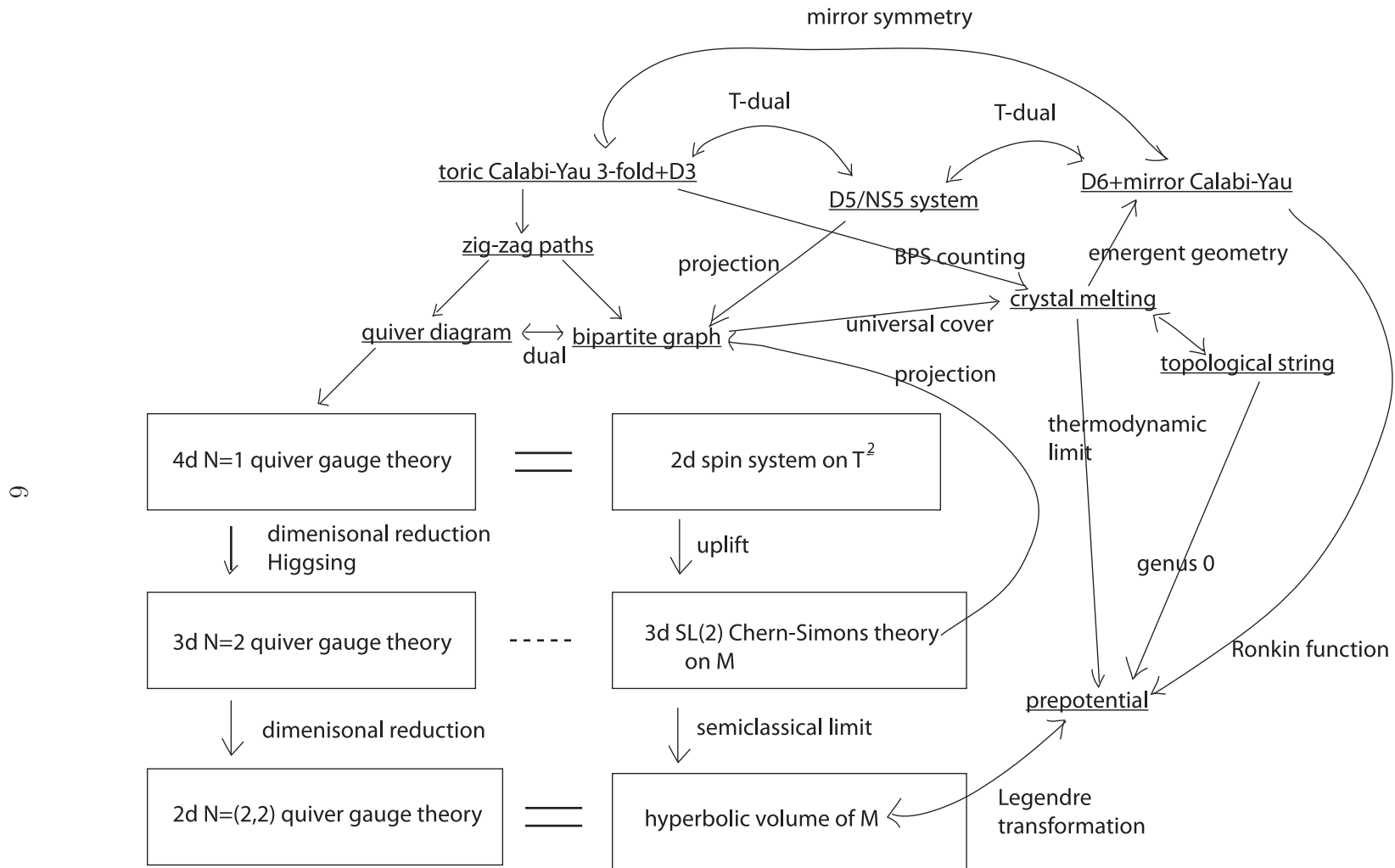


Figure 1: Logical structure of this paper. Clearly it is impossible to list all the connections between all the ingredients mentioned here. The main claims of this paper are the two equalities represented in the center of this figure.

2 Quivers from Zig-Zag Paths

In this section we briefly summarize the construction of 4d $\mathcal{N} = 1$ superconformal quiver theories from “zig-zag paths” on T^2 [2, 32] (see [33, 26] for mathematical formulation). See also the reviews [6, 7] for more details on dimer model techniques.

2.1 Zig-Zag Paths

For the clarity of the presentation let us first explain the combinatorial properties of the zig-zag paths, which is actually rather elementary. The physical context will be explained shortly.

Let us start with a convex polygon Δ in \mathbb{Z}^2 . Geometrically this is the toric diagram for a Calabi-Yau 3-manifold X_Δ , *i.e.*, the cone $\Delta \times \{1\} \in \mathbb{R}^3$ specifies the top-dimensional cone of the fan.

As a toric diagram there are $SL(3, \mathbb{Z})$ ambiguities in the choice of Δ . For example, \mathbb{Z}^2 translation of Δ keeps the geometry. In the following we use the same symbol Δ for the equivalence class of Δ under this identification.

One way to specify Δ is to write down the set of primitive normals of the polygon. Let us denote them by $(r_i, s_i) \neq (0, 0)$ with $i = 1, \dots, d$. We choose the label i such that the direction of the vector p_i rotates in the counterclockwise manner as we increase i . The integer d , which is the number of lattice points in the boundary of Δ , is fixed throughout this paper. Note that in general the same vector could appear multiple times in this list. This happens when an edge at the boundary of Δ contains more than two lattice points.

By definition we have

$$\sum_i r_i = \sum_i s_i = 0 . \tag{2.1}$$

Let us now consider zig-zag paths. The zig-zag paths are a set of closed oriented cycles p_1, \dots, p_d on a two-dimensional torus T^2 , whose homologies cycles are determined by (r_i, s_i) :

$$[p_i] = r_i[\alpha] + s_i[\beta] \in H_1(T^2, \mathbb{Z}) \quad \text{fixed and non-trivial} , \tag{2.2}$$

where $[\alpha], [\beta]$ are the basis of $H_1(T^2, \mathbb{Z})$, for example α and β -cycles of the torus. There is $SL(2, \mathbb{Z})$ ambiguity in the choice of $[\alpha], [\beta]$, which could be absorbed into the $SL(2, \mathbb{Z})$

ambiguity in the choice of Δ . The origin of the terminology “zig-zag path” will be clarified shortly when we study dimer models.

We assume the following three conditions.

- **genericity.** First, we assume that no three paths intersect at a single point (Figure 2). This is satisfied for generic choice of paths.
- **admissibility.** Second, we impose the *admissibility condition* (this terminology comes from [33]). To explain this, let us note that the paths divide the torus into a union of convex polygons. We color the convex polygon by black (white) if all the paths around the polygon has counterclockwise (clockwise) orientation around the polygon; otherwise the face is kept uncolored. The paths are called admissible if every edge bounds a colored polygon (Figure 3).

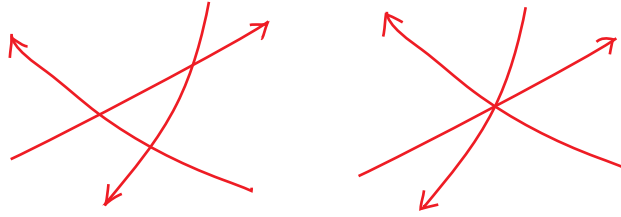


Figure 2: Genericity condition, stating that no three zig-zag paths intersects at a single point. The left figure is allowed, whereas the right is not.

These two conditions are sufficient for the 4d quiver gauge theory. We moreover impose one simplifying assumption

- **minimality.** Minimality (this terminology comes from [26]) forbids the two possibilities shown in Figure 4.

We will come back to the physical significance of the admissibility condition in section 2.3, but for the moment let us first analyze its combinatorial implication by defining graphs on T^2 .

Given a set of zig-zag paths we can define a natural bipartite graph \mathcal{G}^* and its dual \mathcal{G} , both realized on T^2 (the symbol is chosen for later convenience). In the literature \mathcal{G}^* is often called a brane tiling [3, 4, 5], and \mathcal{G} a periodic quiver. The vertices of \mathcal{G}^* are given by colored faces, and the edges by the intersection points between them. The orientation of zig-zag paths gives a natural orientation to the edges, and ensures that

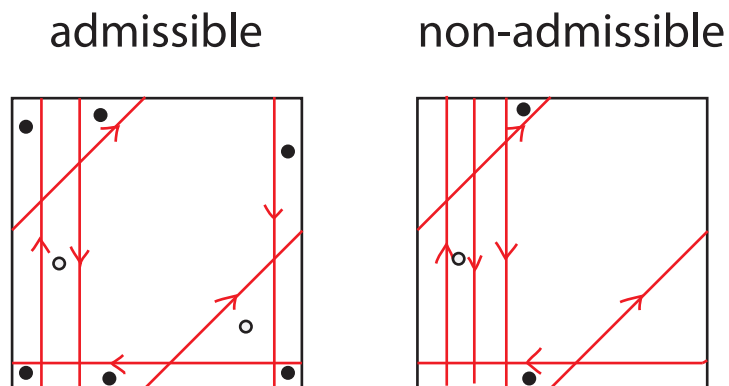


Figure 3: Admissible (left) and non-admissible (right) configuration of zig-zag paths. Rather than coloring the faces by black and white, we have represented the coloring by placing black and white dots inside (it is hard to represent the white color on a white paper!). We see from this example that moving a zig-zag path across an intersection point breaks the admissibility condition.

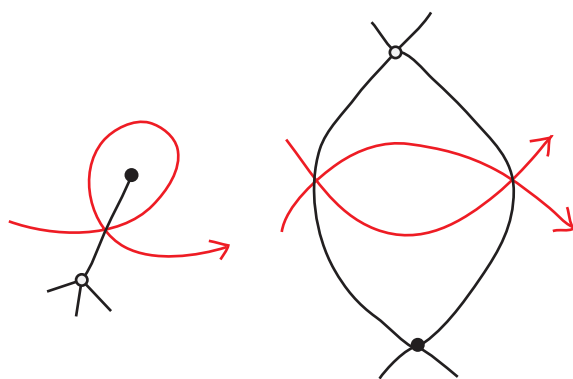


Figure 4: Minimality condition forbids two types of intersections of zig-zag paths. The graph superimposed on it is the bipartite graph \mathcal{G}^* .

the resulting graph is bipartite, *i.e.*, vertices are colored either black or white and edges connect vertices of different colors.

The graph \mathcal{G}^* is dual of \mathcal{G} . This means the vertices are placed on the uncolored faces, and the edges at each intersection point between them. The orientation of the zig-zag paths determine the orientation of the edges. In the following we denote the set of vertices, edges and faces of \mathcal{G} by V, E and F . Since we have black and white colors we have a decomposition into black and white faces: $F = B \cup W$. For an edge $e \in E$ we denote the source (and the target) by $s(e)$ ($t(e)$). Since \mathcal{G} is drawn on T^2 we have

$$|V| - |E| + |F| = 0 . \quad (2.3)$$

We also denote by V^*, E^*, F^* the set of vertices/edges/faces of the graph \mathcal{G}^* . By definition we have

$$V^* = F, \quad E^* = E, \quad F^* = V .$$

We have defined $\mathcal{G}, \mathcal{G}^*$ from zig-zag paths, but we can go in the other direction. Given a bipartite graph we define a zig-zag paths to be graph on \mathcal{G}^* which turns maximally right (left) at black (white) vertex. Because the graph is finite, we always come back to the same vertex after several steps and hence this defines a set of closed loops. The name zig-zag path originates from the zig-zag shape of the path³ (see Figure 5).

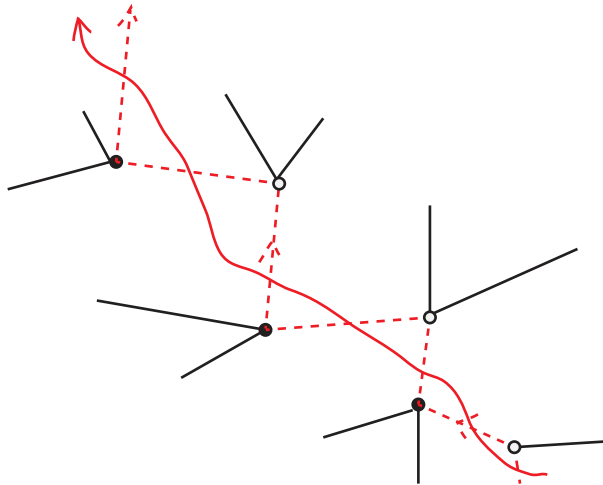


Figure 5: A zig-zag path on the bipartite graph \mathcal{G}^* (dotted path) is identified with the zig-zag path defined previously (undotted arrow).

³This is also called a rhombus loop or a train track in the literature. The word “rhombus” refers to a quadrilateral in Figure 13, which becomes a rhombus for isoradial circle patterns.

We can verify that this gives an inverse to our previous construction, *i.e.*, from the bipartite graph we recover the zig-zag paths we started with. However, it is important to notice that this correspondence is not one-to-one; we can start with an admissible configuration to obtain another configuration by locally applying the two basic moves shown in Figure 6. These two moves are called *fundamental moves* in this paper and complete in the sense that any two minimal bipartite graphs corresponding to the same Δ are related by a sequence of these two moves [26, Theorem 2.5]. The same theorem guarantees the existence of minimal admissible configuration of zig-zag paths. Note that the number of nodes of the quiver is preserved in the fundamental moves.

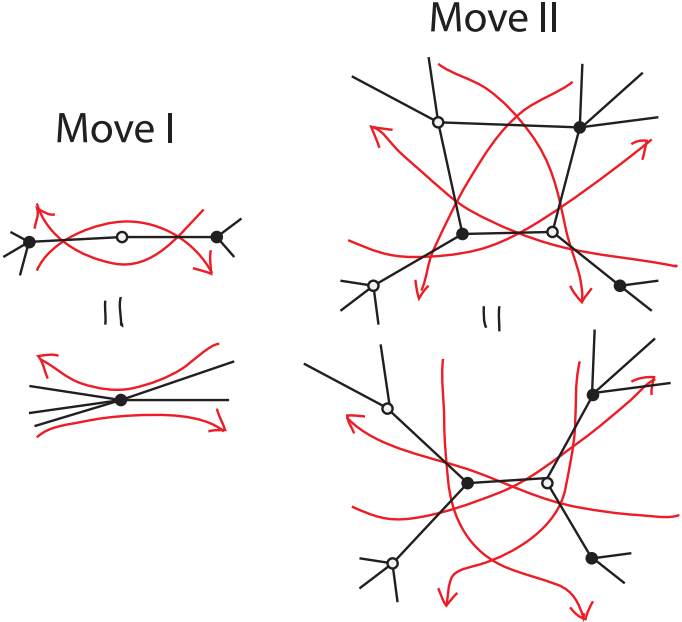


Figure 6: Two basic moves (fundamental moves) preserving the admissibility condition. The second move is called a double Yang-Baxter move.

It should be kept in mind that the choice of the fundamental moves is not unique. For example, we could replace the second move in Figure 7 by a different move, for example the ones shown in Figure 6. We can easily check that these moves, in combination with move I, generate the same set of moves. We call move II' a Seiberg move (it is exactly Seiberg duality, as we will see shortly) and move II'' a spider move. For later reference, we also list basic moves for zig-zag paths without admissibility condition imposed (Figure 8). These are reminiscent of the Reidemeister moves of knot theory.

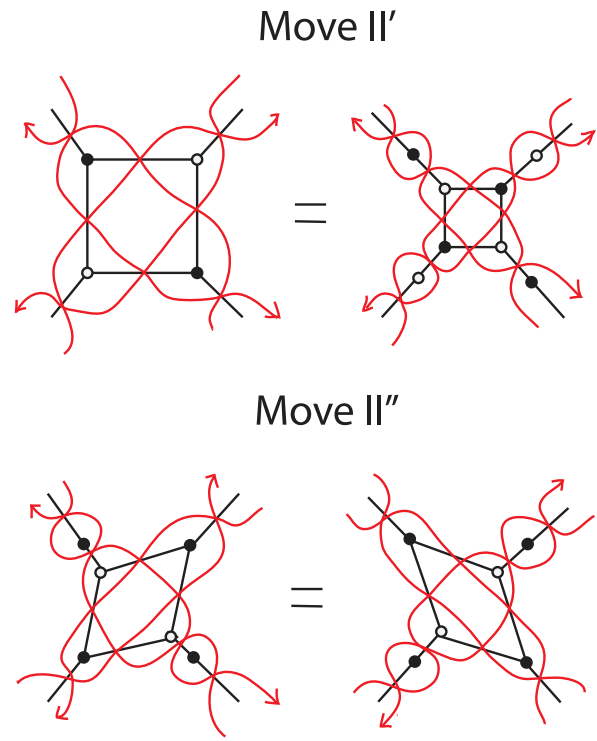


Figure 7: We can replace the fundamental move II in Figure 6 by either of the two moves shown here.

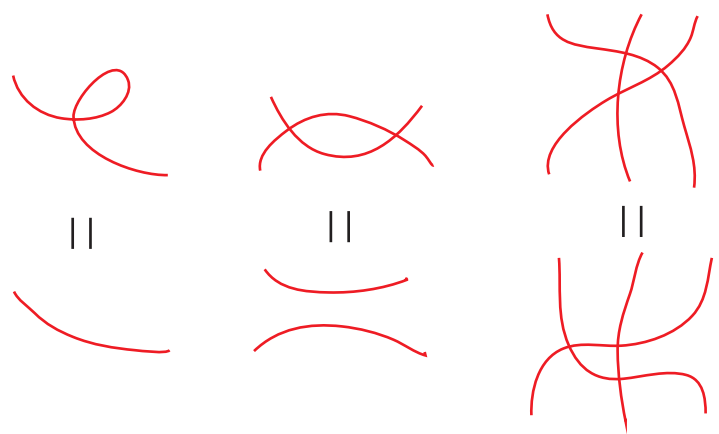


Figure 8: Moves for zig-zag paths without admissibility condition. Here we do not show the orientation of the zig-zag paths, and all orientations are allowed.

2.2 Quiver Gauge Theories

Let us next define 4d $\mathcal{N} = 1$ quiver gauge theories from the combinatorial data of the previous subsection. This is simply a quiver gauge theory determined from \mathcal{G} . In other words, we have a gauge group $SU(N)_v$ for each vertex $v \in V$, and a bifundamental chiral multiplet X_e for each $e \in E$. The total gauge group is given by

$$G = \prod_{v \in V} SU(N)_v . \quad (2.4)$$

Here and in the following we will specialize to the case where the ranks of the gauge groups are all equal to N . Most of the analysis of the next section on 4d superconformal index generalizes straightforwardly to more general cases where the ranks are position dependent. However, the analysis of the Seiberg duality in 4d, and also of the reduction to 3d, requires some change.

We also determine the superpotential to be

$$W = \sum_{b \in B} \text{Tr} \left(\prod_{e \in b} X_e \right) - \sum_{w \in W} \text{Tr} \left(\prod_{e \in w} X_e \right) , \quad (2.5)$$

where the product inside the trace is taken in the counterclockwise (clockwise) manner for B and W .

The quiver gauge theory constructed in this way contains examples with enhanced supersymmetries, for example the $\mathcal{N} = 4$ theory or $\mathcal{N} = 2$ theories corresponding to the A_L type singularities [34]. However, generically the theory is chiral, and has $\mathcal{N} = 1$ supersymmetry. The typical example in the literature is the theory dual to the conifold [35].

Although our theory is in general chiral, there is no chiral anomaly. This is because by construction the number of incoming and outgoing arrows for each vertex $v \in V$ are the same.

The quiver gauge theories constructed in this way is the world-volume effective theory on the D3-branes probing the toric Calabi-Yau manifold X_Δ , and flows in the IR to a non-trivial IR fixed point.

The basic moves in Figure 6 is an operation on quiver gauge theories which keeps the IR fixed point intact [4]. The first move is to remove two fields X, Y with superpotential $\text{Tr}(XY)$ from the theory — because this superpotential term represents a mass term, we can simply integrate out a massive field. The second move (move II') corresponds to a Seiberg duality (see [7], section 4.7 for detailed exposition), or equivalently the mutation of the quiver.

Note that in our setup Seiberg duality can be taken only for those nodes which has four arrows (two incoming and two outgoing). This is because N_f is always a multiplet of N , and the only value of N_f in the conformal window is $N_f = 2N^4$.

Finally, let us comment on a further simplifying assumption on the bipartite graph. A bipartite graph is called isoradial if all the vertices can be placed on circles of equal radius. In terms of zig-zag paths this is satisfied if and only if (1) each zig-zag path is a simple closed curve and (2) the lift of any pair of zig-zag paths to the universal cover intersect at most once [36]. Colloquially this means that all the zig-zag paths are “straight enough” such that the zig-zag paths have minimal intersection numbers. This means that the number of edge of the quiver is minimal, *i.e.*, we have

$$|E| = \sum_{i < j} |\langle p_i, p_j \rangle| = \sum_{i < j} |r_i s_j - r_j s_i| . \quad (2.6)$$

We will see that this condition leads to enormous simplifications of part of the upcoming analysis; for example, in section 4.3 we will comment on this condition in the context of 2d gauge theories. However, it should be kept in mind that isoradiality is not a necessary condition, and for example stronger than the consistency conditions in [32, 37, 38].

2.3 Brane Configuration

The quiver gauge theories in the previous subsection could be realized by D5/NS5 brane configurations [39, 40, 7]. Let us briefly summarize this, since this clarifies the origin of the apparently ad hoc assumptions in the previous subsection.

The relevant brane configuration is

		0	1	2	3	4	5	6	7	8	9	
N D5		-	-	-	-		.		.			
NS5		-	-	-	-		Σ					

(2.7)

Here N D5-branes wraps the T^2 along the 57 directions, whereas a single NS5-brane wraps a holomorphic cycle Σ in 4567 direction. If we write $x = e^{x_4 + ix_5}$, $y = e^{x_6 + ix_7}$, then the holomorphic curve is given by

$$\Sigma = \{P(x, y) = 0\} \subset (\mathbb{C}^\times)^2 , \quad (2.8)$$

⁴ It is important that not all the possible mutations of the quiver physically make sense. If we mutate on the n -valent vertex with $n \geq 6$, the result is in general a graph which could not be realized on torus.

where P the so-called Newton polynomial of Δ , defined by

$$P(x, y) = \sum_{(i,j) \in \Delta} c_{i,j} x^i y^j . \quad (2.9)$$

with generic coefficients $c_{i,j}$. Here $(i, j) \in \Delta$ means the lattice point (i, j) is a lattice point of Δ (including the boundary). The curve Σ is a Riemann surface of genus g and puncture d , where g is the number of internal lattice points inside Δ (recall that d also denotes the number of zig-zag paths in section 2.1). This curve is part of the mirror \check{X}_Δ of the toric Calabi-Yau 3-fold X_Δ given by [41, 42]

$$\check{X}_\Delta : uv + P(x, y) = 0 , \quad (2.10)$$

with $u, v \in \mathbb{C}$. We will encounter $P(x, y)$ again as a spectral curve of the dimer model. The identification of the NS5-brane curve and the mirror curve could be explained by a T-duality, where our D5/NS5 system is mapped to a configuration of D6-branes wrapping Lagrangian 3-cycles inside \check{X}_Δ [43].

This brane configuration can be looked at from two different ways: D5-brane viewpoint and the NS5-brane viewpoint. In the former, we have a T^2 , which is the torus we had previously, and the zig-zag paths represent the intersection cycles of an NS5-brane and the D5-brane; and the colored faces represents the projection of the shape of the NS5-brane. In this language, the colored regions correspond to the projection of the mirror curve into the 57 directions (called coamoeba/alga [43]), and the black/white color represents the orientation of the curve when projected onto T^2 . In other words, black/white regions represents $(N, 1)/(N, -1)$ -branes, and uncolored regions $(N, 0)$ -branes. This explains why $U(N)$ gauge group lives in uncolored regions. The bifundamental fields originate from the massless strings between the $U(N)$ gauge groups, namely the intersection points of the uncolored regions. The admissibility condition simply says we do not have (N, k) -branes with $|k| \geq 2$, in which case no Lagrangian descriptions are known.

We could also take the NS5-brane viewpoint. Then we have a Riemann surface Σ , on which we have a set of 1-cycles representing the intersection with D5-branes. Our Riemann surface Σ is reconstructed as the surface whose boundaries are the cycles of zig-zag paths [43]. This is parallel to the construction of the Seifert surface in knot theory, and Seiberg duality in the original graph is translated into the half Dehn twist of Σ [26]. We will encounter this Riemann surface Σ again in section 4.5.

2.4 R-charges

We are going to consider the IR fixed point of our quiver gauge theories. Due to the strong coupling effects the bifundamental chiral multiplets could have large anomalous dimensions in the IR. This is determined from the IR $U(1)_R$ R-symmetry in the superconformal algebra. In general, it is a rather non-trivial problem to identify the IR superconformal R-symmetry $U(1)_R$, because UV R-symmetry mixes with the global UV $U(1)$ symmetries. Here we will comment on one particular useful parametrization of the UV global symmetry or equivalently IR R-symmetry (see [2, 39, 40]⁵).

We are going to define d global symmetries, with 1 relation among them. For each zig-zag path p_i , let us define the charge of the bifundamental field X_e at an edge $e \in E$ by

$$Q_i[X_e] = \langle p_i, e \rangle, \quad (2.11)$$

where the bracket here refers to the (signed) intersection number of the two paths p_i and e . To see that this is in fact a global symmetry, recall that a term in the superpotential is represented by a closed loop around a black/white vertex of the bipartite graph (see (2.5)), and has 0 intersection number with a closed loop p_i . Because two zig-zag paths pass through e with an opposite orientation, we find that the diagonal subgroup of these d global symmetries is trivial (see 2.1)

$$\sum_i Q_i[X_e] = 0. \quad (2.12)$$

Hence we find $d - 1$ global symmetries. These symmetries are anomaly free [44], because

$$\sum_{e: \text{around } v} Q_i[X_e] = 0 \quad \text{for all } i. \quad (2.13)$$

This holds because a zig-zag path incoming to a vertex necessarily goes out of the vertex, with an opposite orientation and hence with a field with an opposite flavor charge.

It is known that generically this parametrization exhausts all the possible global symmetries⁶. There is a corresponding statement in the AdS dual; two out of $d - 1$ correspond to isometries of the Sasaki-Einstein manifold and called mesonic symmetries, whereas the remaining $d - 3$ symmetries are associated with the 3-cycle of the Sasaki-Einstein manifold and called baryonic symmetries.

⁵The paper [2] discuss the case of isoradial bipartite graphs, however our parametrization applies to more general bipartite graphs. This will be crucial when we discuss Seiberg duality in section 3.2.

⁶In some special cases there could be an enhancement to non-Abelian global symmetries.

We can also describe R-symmetries. The choice of UV R-symmetry is not unique, since we can consider a mixing with the $d - 1$ global symmetries mentioned above (the IR R-symmetry inside superconformal algebra is determined by a-maximization [45]).

For our purpose, a particularly useful parametrization is given as follows. Let us choose a set of d parameters θ_i for each zig-zag path p_i , and let us assume that they are defined modulo 2π ($\theta_i \sim \theta_i + 2\pi$), and that $0 \leq \theta_{i+1} - \theta_i \leq \pi$ for all i ($\theta_{d+1} := \theta_1$). We can regard θ_i as the slope of p_i . Then for each bifundamental X_e for $e \in E$ its R-charge is simply defined to be the relative slopes of the two zig-zag paths which goes through the edge. More formally, we define

$$R_e = R[X_e] := \frac{1}{\pi} \text{sign}\langle p_{L(e)}, p_{R(e)} \rangle [\theta_{L(e)} - \theta_{R(e)}] , \quad (2.14)$$

where $[x]$ denotes a real number in $[0, 2\pi]$ and equivalent to x modulo 2π . We also used the notation that a chiral multiplet corresponding to an edge e has a flavor charge $+1$ for the $L(e)$ -th zig-zag path and -1 for the $R(e)$ -th path, where $p_{L(e)}$ and $p_{R(e)}$ are two zig-zag paths passing through e from opposite sides (see Figure 9). From the definition we have $R_e \geq 0$.

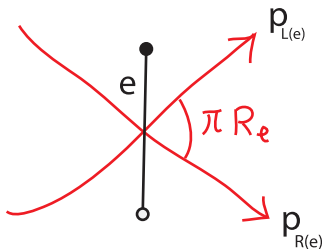


Figure 9: An bifundamental at an edge e has flavor charge $+1$ for $L(e)$ -th flavor charge and -1 for $R(e)$ -th flavor charge, where $p_{L(e)}, p_{R(e)}$ are two zig-zag paths as in this Figure.

We have the following two conditions on IR R-symmetries.

- First, the β -function for Yukawa couplings vanish. This is the same as the requirement that the R-charge of the superpotential, and therefore any term in the superpotential, is normalized to be 2. This means

$$\sum_{e \in F} R_e = 2 . \quad (2.15)$$

- Second, the β -functions for the gauge coupling vanish. From the NSVZ β -function, which in our case could be written as

$$\frac{d}{d \log \mu} \frac{1}{g_v^2} = \frac{N}{1 - g_v^2 N / 8\pi^2} \left[3 - \frac{1}{2} \sum_{e \in v} (1 - \gamma_e) \right] , \quad (2.16)$$

where the anomalous dimension γ_e is related to the R-charge by $\gamma_e = 3R_e - 2$. From this condition, we have

$$\sum_{e \in V} (1 - R_e) = 2 . \quad (2.17)$$

This can be written more symmetrically

$$\sum_{e \in F^*} R_e^* = 2 , \quad (2.18)$$

where we defined $R_e^* := 1 - R_e$.

These two conditions follow from the definition (2.14) and the fact that the sum of exterior angles of a polygon is 2π .

Naively the dimension of the solution space to (2.15), (2.17) is zero because we have $|E|$ parameters R_e and $|V| + |F|$ constraints (see (2.3)). However, in supersymmetric theories not all the constraints are independent and it has been demonstrated that the solution has $d - 1$ parameters [40]. Again, it is straightforward to see that the two conditions (2.15), (2.18) are preserved under the deformation with the $d - 1$ parameters. Of course, this is the same as the number of global symmetries treated above.

3 Superconformal Index As Spin System

In this section we first define the superconformal index for 4d $\mathcal{N} = 1$ superconformal gauge theories. We then show that the 4d index for the spin system defined in previous section is equivalent to the partition function of a spin system on T^2 .

3.1 Superconformal Index

The Definition

Let us consider 4d $\mathcal{N} = 1$ superconformal theory on $S^1 \times S^3$. This theory has supercharges $\mathcal{Q}_\alpha, \bar{\mathcal{Q}}_{\dot{\alpha}}$ and $\mathcal{S}_\alpha, \bar{\mathcal{S}}_{\dot{\alpha}}$, where α and $\dot{\alpha}$ denotes the spins $SU(2)_1$ and $SU(2)_2$ of the isometry of S^3 : $Spin(4) = SU(2)_1 \times SU(2)_2$. To define an index, we need to pick up a particular supercharge. There are four supercharges, but \mathcal{Q}_+ and \mathcal{Q}_- ($\bar{\mathcal{Q}}_+$ and $\bar{\mathcal{Q}}_-$) define the same index due to the $SU(1)_1$ ($SU(2)_2$) symmetry, and hence we have two possibilities. When we choose $\mathcal{Q} = \mathcal{Q}_-$, the superconformal index is defined as an index defined from \mathcal{Q} , with insertions of operators commuting with \mathcal{Q} :

$$I^L(t, y; z) = \text{Tr} \left[(-1)^F t^{2(\mathcal{E}+j_2)} y^{2j_1} u^{\mathcal{F}} e^{-\gamma\{\mathcal{Q}, \mathcal{Q}^\dagger\}} \right] , \quad (3.1)$$

where the index is taken over the Hilbert space on S^3 . F is the fermion number, \mathcal{E} is the energy, j_1 and j_2 are the spins of $SU(2)_1$ and $SU(2)_2$, respectively, and $u^{\mathcal{F}} := \prod_i u_i^{\mathcal{F}_i}$, where \mathcal{F}_i (u_i) is the charge (chemical potential) under the i -th flavor symmetry⁷. Note that due to the translation symmetry we could flip the sign of j_1 , and we have

$$I^L(t, y; u) = I^L(t, y^{-1}; u) . \quad (3.2)$$

This index, often called the left-handed index (hence the symbol L in (3.1)) is independent of the value of γ thanks to the standard index argument, and can be computed in the limit $\gamma \rightarrow \infty$

$$I^L(t, y; u) = \text{Tr} [(-1)^F t^{2(\mathcal{E}+j_2)} y^{2j_1} u^{\mathcal{F}}] , \quad (3.3)$$

where the trace is now taken over all states satisfying

$$\{\mathcal{Q}, \mathcal{Q}^\dagger\} = \mathcal{E} - 2j_2 + \frac{3}{2}r = 0 , \quad (3.4)$$

where r is the $U(1)$ R-charge. Similarly, if we choose $\overline{\mathcal{Q}} = \overline{\mathcal{Q}}_-$, we can define the right-handed index

$$I^R(t, y; u) = \text{Tr} [(-1)^F t^{2(E+j_1)} y^{2j_2} u^{\mathcal{F}}] , \quad (3.5)$$

where the trace is taken over all states satisfying

$$\{\overline{\mathcal{Q}}, \overline{\mathcal{Q}}^\dagger\} = E - 2j_1 - \frac{3}{2}r = 0 . \quad (3.6)$$

This is the same as the left-handed index, except that the orientation of the arrows of the quiver diagrams are reversed. Since this can be taken into account by a change of convention, in the following we will concentrate on the left-handed index and denote the corresponding index simply by I .

For our later purposes it is useful to reparametrize the chemical potentials as

$$p = t^3 y, \quad q = t^3 y^{-1} . \quad (3.7)$$

In this notation, the superconformal index reads

$$I^L(p, q; u) = \text{Tr} \left[(-1)^F p^{\frac{E+j_2}{3}+j_1} q^{\frac{E+j_2}{3}-j_1} u^{\mathcal{F}} e^{-\gamma\{Q, Q^\dagger\}} \right] . \quad (3.8)$$

One subtlety we have is that our 4d quiver theory is defined in UV, and is conformal only in the IR, where the theory is strongly coupled. Because the index is independent

⁷This is often denoted by z_i in the literature.

of the continuous parameter, it is independent of the dimensionless parameter obtained by multiplying the energy scale by the radius of S^3 , and we could compute the index in UV, except that we have to take into account the mixing of UV R-symmetry with global symmetry. In our analysis this is taken into account when we have included chemical potentials for global symmetries. In practice this means that the effect of anomalous dimensional could be taken into effect by shifting the global symmetry chemical potentials by powers of t .

Integral Expression

Because an index is invariant under the continuous deformation of parameters of the Lagrangian, the superconformal index can be computed by taking the free field limit. Alternatively, we could apply localization techniques. In either way, the result is written as an integral over the Cartan of the Cartan H of the gauge group, which in our case is given by

$$H = (\mathrm{U}(1)^{N-1})^{|V|} \subset G = \mathrm{SU}(N)^{|V|} . \quad (3.9)$$

We parametrize an element of the Cartan of $\mathrm{SU}(N)_v$ (at vertex $v \in V$) by $z_v = (z_{v,1}, \dots, z_{v,N})$ satisfying $\prod_{i=1}^N z_{v,i} = 1$. We also write $z_{v,i} = e^{i\sigma_{v,i}}$, where $\sigma_{v,i}$ is periodic with period 2π . Physically these parameters represents the Polyakov loop along the thermal direction S^1 .

The index is expressed in a plethystics form (this follows from group theory, see [10])

$$I(p, q, u) = \int \prod_{v \in V} \left[d\mu_v \prod_{i < j} (z_{v,i} - z_{v,j})(z_{v,i}^{-1} - z_{v,j}^{-1}) \right] \exp \left(\sum_{n=0}^{\infty} i(p^n, q^n, u^n; z^n) \right) \quad (3.10)$$

Here the integration measure contains $d\mu_v$ defined by

$$d\mu_v = \frac{1}{N!} \prod_{i=1}^{N-1} \frac{dz_v}{2\pi i z_v} , \quad (3.11)$$

as well as the Vandermonde determinant, and the integral over the contour $|z_{v,i}| = 1$ (or $\sigma_{v,i}$ runs from 0 to 2π). The ‘‘single-letter index’’ $i(p, q, u; z)$ is given as a sum over contributions from vector and chiral multiplets

$$i(p, q, u; z) = \sum_{v \in V} i_{\mathrm{vect}}^v(p, q; z) + \sum_{e \in E} i_{\mathrm{chiral}}^e(p, q, u; z) , \quad (3.12)$$

where

$$i_{\text{vect}}^v(p, q; z) = \left[1 - \frac{1 - pq}{(1 - p)(1 - q)} \right] \chi_{\text{adj}}(z_v), \quad (3.13)$$

$$i_{\text{chiral}}^e(p, q, u; z) = \frac{1}{(1 - p)(1 - q)} \left[(pq)^{\frac{R_e}{2}} y u_{L(e)} u_{R(e)}^{-1} \chi_{\text{bifund}}(z_{s(e)}, z'_{t(e)}) \right. \\ \left. - (pq)^{1 - \frac{R_e}{2}} / (y u_{L(e)} u_{R(e)}^{-1}) \chi_{\text{bifund}}(z_{s(e)}^{-1}, z'_{t(e)}^{-1}) \right], \quad (3.14)$$

and χ_{adj} and χ_{bifund} are the characters for the adjoint and bifundamental representations, respectively

$$\chi_{\text{adj}}(z) = \sum_{1 \leq i, j \leq N} (z_i z_j^{-1}) - 1, \quad \chi_{\text{bifund}}(z, z') = \sum_{i, j=1}^N z_i z_j'^{-1}. \quad (3.15)$$

Note that vector multiplets are not charged under flavor symmetries.

For our purposes, it is useful to rewrite the index in a different form

$$I(p, q, u) = \int \prod_{v \in V} d\mu_v \left(\prod_{v \in V} I_{\text{vect}}^v(p, q; z) \right) \left(\prod_{e \in E} I_{\text{chiral}}^e(p, q, u; z) \right), \quad (3.16)$$

where

$$I_{\text{vect}}^v(p, q; z) = \kappa(p, q)^{N-1} \prod_{k \neq l} \frac{1}{\Gamma(z_{v,k} z_{v,l}^{-1}; p, q)}, \quad (3.17)$$

and

$$I_{\text{chiral}}^e(p, q; z) = \prod_{1 \leq k, l \leq N} \Gamma((pq)^{\frac{R_e}{2}} u_{L(e)} u_{R(e)}^{-1} z_{s(e),k} z_{t(e),l}^{-1}; p, q). \quad (3.18)$$

Here $\Gamma(z; p, q)$ is the elliptic gamma function defined in (A.1) and we defined (see (A.5))

$$\kappa(p, q) := (p; p)_{\infty} (q; q)_{\infty}. \quad (3.19)$$

The equivalence of the two expressions (3.10) and (3.16) can be verified by the equations of the form

$$\exp \left(\sum_{n=1}^{\infty} \frac{1}{1 - x^n} \right) = \prod_{m=0}^{\infty} \frac{1}{1 - x^m}. \quad (3.20)$$

and the equalities in Appendix, for example (A.8).

We here obtained the expression of the index (3.16) by rewriting (3.10). However it should be emphasized that (3.16) arises directly in the localization derivations of the

index (see for example [46] and [29, Appendix]). The factors I_{vect}^v (I_{matter}^e) represents the 1-loop determinants for vector multiplet at vertex v (chiral multiplet at edge e), and the infinite product comes from the spherical harmonics expansion on S^3 . In the free field computation, we have the S^3 Laplacian from the bosons, whose determinant could be written as products over the quantum numbers of the spherical harmonics, and the same applies to fermions. There are cancellations between bosons and fermions, and the unpaired bosonic (fermionic) modes appear in the denominator (numerator) of the product (A.1).

3.2 Invariance under Fundamental Moves

In this section we prove an invariance the superconformal index under the fundamental moves. The general argument that the 4d index depends only at the IR fixed point guarantees this invariance, but we can also check this explicitly.

Generalities on Gluing

It is important to note that the two fundamental moves in Figure 6 are local operations on the quiver diagram. We therefore expect that the invariance of the index should reduce to the invariance of the index defined for the subdiagram.

To formalize this idea we need to invoke the concept of “gluing” in gauge theories. Let us first explain this in a rather general situation⁸. Consider two 4d $\mathcal{N} = 1$ theories T_1 and T_2 which has global symmetries G_1 and G_2 . Suppose moreover that these flow in the IR to non-trivial fixed points. We can then compute the superconformal indices for each of these theories, with the chemical potentials for global symmetries included.

Now from the two global symmetries G_1 and G_2 we choose a common subgroup H ($H_1 \subset G_1$, $H_2 \subset G_2$, $H \simeq H_1 \simeq H_2$) and gauge H , *i.e.*, the diagonal subgroup of $H_1 \times H_2$. The resulting theory has global symmetry $G_1 \backslash H_1 \times G_2 \backslash H_2$, where $G \backslash H$ denotes the commutant of H inside G , see Figure 10.

This gluing operation has a counterpart at the level of the index. Let us denote the indices of T_1 and T_2 by $I_1(p, q; u_1, w)$ and $I_2(p, q; u_2, w)$, where u_1 and u_2 denotes the chemical potentials for the Cartan of the flavor symmetries $G_1 \backslash H_1$ and $G_2 \backslash H_2$, respectively, and w for those for H . We then have⁹

$$I(p, q; u_1, u_2) = \int \frac{dw}{2\pi iw} \int I_1(p, q; u_1, w) I_{\text{vect}}(w) I_2(p, q; w, u_2) . \quad (3.21)$$

⁸This discussion obviously generalizes to quantum field theories in other dimensions, for example to ellipsoid partition function in 3d studied in section 4.1.

⁹This is the gluing of “generalized index”, see [47] for similar analysis in 3d.

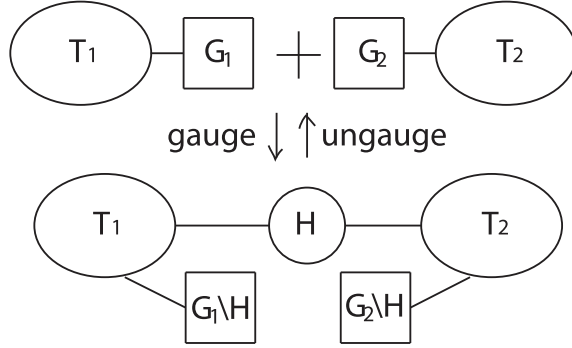


Figure 10: We can glue two theories T_1 and T_2 by gauging a common global symmetry H .

Note that after gluing the global symmetry is promoted to dynamical degrees of freedom to be integrated over, and hence we have included the 1-loop determinant for w .

Let us apply this to our case, where one of our moves replaces a quiver diagram with another. Since the fundamental moves are local operations on the graph, we could decompose the quiver diagram Γ into two parts along edges of Γ such that Γ_1 becomes Γ_2 after the move and $\Gamma \setminus \Gamma_1 = \Gamma \setminus \Gamma_2$ kept intact. Then the rule in (3.21) immediately gives

$$I_\Gamma = \int d\mu(z) I_{\text{vect}}(p, q) I_{\Gamma_1}(p, q; z) I_{\Gamma/\Gamma_1}(p, q; z) , \quad (3.22)$$

and

$$I_{\Gamma'} = \int d\mu(z) I_{\text{vect}}(p, q) I_{\Gamma_2}(p, q; z) I_{\Gamma/\Gamma_2}(p, q; z) . \quad (3.23)$$

The equality of these two quantities follow if we could show the local invariance of the index

$$I_{\Gamma_1} = I_{\Gamma_2} . \quad (3.24)$$

Because any duality is generated by combination of the two moves (section 2.1), all we need to do is to check the invariance under the two fundamental moves.

Integrating Out

Let us first study move I. After the move we have two extra bifundamental fields X_1 and X_2 between two gauge group $SU(N)_v$ and $SU(N)_{v'}$, which has a superpotential

term $\text{Tr}(X_1 X_2)$. This means that the sum of R-charges is two and their global symmetries charges have opposite signs, and the contribution from the two is

$$\Gamma((pq)^{R_e/2} z_v z_{v'}^{-1} u_i u_j^{-1}; p, q) \Gamma((pq)^{(2-R_e)/2} z_{v'} z_v^{-1} u_i^{-1} u_j; p, q) . \quad (3.25)$$

But this is trivial due to (A.2).

Seiberg Duality

Let us first analyze move II', which is equivalent to the Seiberg duality. The invariance of the index under Seiberg duality has been verified in [48]. However, an extra analysis is required here because the invariance of the index holds only for particular assignment of R-charges to fields, and we need to check that the assignment of the R-charge in section 2.4 satisfies this condition.

As we demonstrated already we can concentrate on the part of the bipartite graph which changes under the duality. Let us label the fields of the electric theory by X_i and the magnetic theory by Y_i, Z_i ($i = 1, \dots, 4$) (see Figure 11). Following the rule (2.14) and using the quantity

$$R_{ij} := \frac{1}{\pi} \text{sign}\langle p_i, p_j \rangle [\theta_i - \theta_j] , \quad (3.26)$$

we can parametrize the R-charges as

$$R[X_1] = R_{12}, \quad R[X_2] = R_{41}, \quad R[X_3] = R_{34}, \quad R[X_4] = R_{23} , \quad (3.27)$$

in the electric theory and

$$\begin{aligned} R[Y_1] = R_{34}, \quad R[Y_2] = R_{23}, \quad R[Y_3] = R_{12}, \quad R[Y_4] = R_{41} , \\ R[Z_1] = R_{42}, \quad R[Z_2] = R_{31}, \quad R[Z_3] = R_{24}, \quad R[Z_4] = R_{13} . \end{aligned} \quad (3.28)$$

in the magnetic theory. Note that there are relations

$$R[X_1] = R[Y_3], \quad R[X_2] = R[Y_4], \quad R[X_3] = R[Y_1], \quad R[X_4] = R[Y_2] , \quad (3.29)$$

and

$$\begin{aligned} R[Z_1] = R[X_1] + R[X_2], \quad R[Z_2] = R[X_2] + R[X_3], \\ R[Z_3] = R[X_3] + R[X_4], \quad R[Z_4] = R[X_4] + R[X_1] . \end{aligned} \quad (3.30)$$

The last four equations are natural since Z_i is the meson composed of two electric quarks X_i 's.

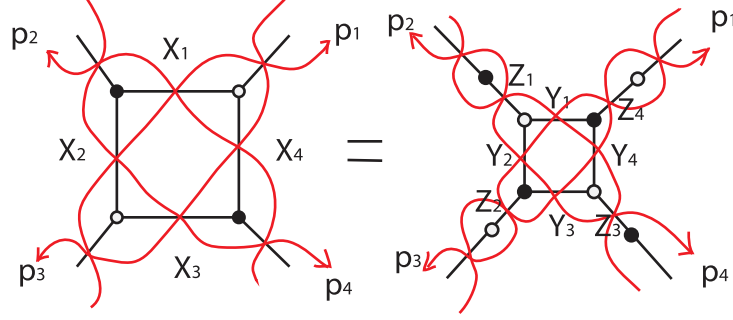


Figure 11: The labeling scheme for the bifundamental fields and zig-zag paths for Seiberg dual theories.

Let us compute the superconformal index. The standard Seiberg duality claims that electric and magnetic theories flow to the same IR fixed point. In the electric theory we have $SU(N)$ gauge theory with $N_f = 2N$ flavors. This theory has in general $SU(N_f) \times SU(N_f)$ flavor symmetries, but in our case we choose $SU(N)^4$ subgroup and denote the chemical potentials by $(s_{1,i}, s_{2,i})$ for fundamental flavors and $(t_{1,i}, t_{2,i})$ for antifundamental flavors ($i = 1, \dots, N$), satisfying $\prod_i s_{k,i} = \prod_i t_{k,i} = 1$ for $k = 1, 2$. From the rule of the previous subsection the index is

$$I_E(p, q) = \frac{\kappa(p, q)^{N-1}}{N!} \int \prod_{i=1}^{N-1} \frac{dz_j}{2\pi i z_j} \frac{\prod_{i=1}^N \prod_{a=1}^{2N} \Gamma(S_a z_j; p, q) \Gamma(T_a z_i^{-1}; p, q)}{\prod_{i \neq j} \Gamma(z_i z_j^{-1}; p, q)}, \quad (3.31)$$

for

$$\begin{aligned} \{S_a\} &= \left\{ (pq)^{\frac{R[X_1]}{2}} s_{1,i} u_1 u_2^{-1}, \quad (pq)^{\frac{R[X_3]}{2}} s_{2,i} u_3 u_4^{-1} \right\}, \\ \{T_a\} &= \left\{ (pq)^{\frac{R[X_2]}{2}} t_{1,i}^{-1} u_4 u_1^{-1}, \quad (pq)^{\frac{R[X_4]}{2}} t_{2,i}^{-1} u_2 u_3^{-1} \right\}. \end{aligned} \quad (3.32)$$

The magnetic theory is again has $SU(N)$ gauge group with $2N$ flavors, and the index contains contributions from mesons:

$$I_M = \frac{\kappa(p, q)^{N-1}}{N!} \prod_{a,b=1}^{2N} \Gamma(\tilde{U}_{a,b}; p, q) \int \prod_{i=1}^{N-1} \frac{dz_j}{2\pi i z_j} \frac{\prod_{i=1}^N \prod_{a=1}^{2N} \Gamma(\tilde{S}_a z_j; p, q) \Gamma(\tilde{T}_a z_i^{-1}; p, q)}{\prod_{i \neq j} \Gamma(z_i z_j^{-1}; p, q)}, \quad (3.33)$$

for

$$\begin{aligned} \{\tilde{S}_a\} &= \left\{ (pq)^{\frac{R[Y_1]}{2}} s_{1,i}^{-1} u_3 u_4^{-1}, \quad (pq)^{\frac{R[Y_3]}{2}} s_{2,i}^{-1} u_1 u_2^{-1} \right\}, \\ \{\tilde{T}_a\} &= \left\{ (pq)^{\frac{R[Y_2]}{2}} t_{1,i} u_2 u_3^{-1}, \quad (pq)^{\frac{R[Y_4]}{2}} t_{2,i} u_4 u_1^{-1} \right\}. \end{aligned} \quad (3.34)$$

and

$$\{\tilde{U}_{a,b}\} = \left\{ (pq)^{\frac{R[Z_1]}{2}} s_{1,i}^{-1} t_{1,i} u_4 u_2^{-1}, (pq)^{\frac{R[Z_2]}{2}} s_{2,i}^{-1} t_{1,i} u_3 u_1^{-1}, \right. \\ \left. (pq)^{\frac{R[Z_3]}{2}} s_{2,i}^{-1} t_{2,i} u_2 u_4^{-1}, (pq)^{\frac{R[Z_4]}{2}} s_{1,i}^{-1} t_{2,i} u_1 u_3^{-1} \right\}. \quad (3.35)$$

What we want to prove is the equivalence of the two expressions

$$I_E(p, q) = I_M(p, q). \quad (3.36)$$

As in [48], we will establish this with the help of a remarkable identity of elliptic hypergeometric functions proven by [49], which is one of the many identities studied, for example, in [50, 51].

In order to apply [49], we need to check the ‘‘balancing condition’’. To state this, define

$$S := \left(\prod_a S_a \right)^{1/N} = (pq)^{\frac{R[X_1] + R[X_3]}{2}} u_1 u_2^{-1} u_3 u_4^{-1}, \\ T := \left(\prod_a T_a \right)^{1/N} = (pq)^{\frac{R[X_2] + R[X_4]}{2}} u_1^{-1} u_2 u_3^{-1} u_4. \quad (3.37)$$

The balancing condition states that

$$ST = pq, \quad (3.38)$$

which follows from the expression for S and T above. In this case we have $I_E = I_M$, provided

$$\tilde{S}_a = S/S_a, \quad \tilde{T}_a = T/T_a, \quad \tilde{U}_{a,b} = S_a T_b. \quad (3.39)$$

These conditions follow from the equalities (3.29), (3.30).

It should also be kept in mind that to establish the identity above (3.36) we do not need to know the exact values of the R-charges determined from a-maximization; the equality of the index holds before a-maximization.

3.3 Z-invariant Spin System

We next show that the superconformal index for our quiver gauge theory can be reformulated as a classical spin model on a lattice in T^2 .

The basic idea is simple. Let us first regard the integral variables $\sigma^v = (\sigma_1^v, \dots, \sigma_N^v)$ as a N -component continuous spin variable at vertex $v \in V$ (recall that these parameters

are related to z_v by $z_v = e^{i\sigma_v}$. These variables are circle valued with period 2π , and in the $SU(N)$ case the N components satisfy a constraint $\sum_{i=1}^N \sigma_i^v = 0$.

Next we need the Boltzmann weights associated with spin configurations. This is determined from the 1-loop determinant I_{vect}^v and I_{chiral}^e :

$$I_{4d} = Z_{\text{spin}} = \int \left(\prod_e d\sigma_e \right) e^{-\sum_{e \in E} \mathcal{E}_e[\sigma] - \sum_{v \in V} \mathcal{E}_v[\sigma]}, \quad (3.40)$$

where we introduced a new expression

$$e^{-\mathcal{E}_v} = I_{\text{vector}}^v, \quad e^{-\mathcal{E}_e} = I_{\text{chiral}}^e. \quad (3.41)$$

In this language, I_{vect}^v is regarded as the self-intersection of the spins at position $v \in V$, and the latter, I_{chiral}^e , is the nearest-neighbor interaction of the spins at positions $s(e), t(e) \in V$.

To some readers this might look like a trivial re-naming of what we already know. However, first note that it is not true for general quiver gauge theories that resulting spin system is realized on T^2 ; the assumption of toric Calabi-Yau dual was crucial for this fact. Second, what is surprising about this spin system is that it is integrable. One simple way to see this is that the invariance of the index under the move II is the invariance of the partition function of the spin system under the double Yang-Baxter move, and the invariance under the Yang-Baxter move is one form of the integrability of the model. The chemical potentials of the 4d index (p, q, u) are regarded as the rapidity variables. In fact, the spin system constructed above coincides with the spin system studied by Bazhanov and Sergeev (hereafter BS) [11, 12], modulo some differences mentioned below.

One technical difference is that the BS model are defined on the plane \mathbb{R}^2 , whereas our model is defined on T^2 . Another more essential difference is that the integrable models have an invariance under a single Yang-Baxter move, whereas our index has an invariance only under the double Yang-Baxter move.

Let us here explain this difference in more detail. In the BS model, to realize a single Yang-Baxter move we have to abandon the admissibility condition on zig-zag paths. Even in this case we could still choose a checkerboard pattern for the faces, corresponding to the colored and uncolored faces in our previous discussion. More concretely, in the brane realization explained in section 2.3 regions with (N, k) -brane with k even (k odd) are colored (uncolored). We associate the spin variables $\sigma_{v,i}$ to uncolored regions, where $i = 1, \dots, N$ and v is the label for the uncolored region.

To define the Boltzmann weight, first we define the self energy $e^{-\mathcal{E}_v^{\text{BS}}[\sigma]}$ as before. The definition of the nearest neighbor interaction $e^{-\mathcal{E}_e^{\text{BS}}[\sigma]}$ is more tricky, since in this general

case we have two different types of edges, shown in Figure 12. For the two possibilities BS model assigns two different weights, which was denoted by \mathcal{W} and $\overline{\mathcal{W}}$.

What BS has shown is that for a judicious choice of $\mathcal{E}_v^{\text{BS}}$ and $\mathcal{E}_e^{\text{BS}}$, the model is integrable and is invariant under moves shown in Figure 8, including the single Yang-Baxter move. For $N = 2$ the weight satisfies the star-triangle relation, and this reduces to Spiridonov's formula for the elliptic hypergeometric function [52]. For $N > 2$, the start-star relation is still a conjecture, although there is non-trivial evidence from power series expansion, see [11].

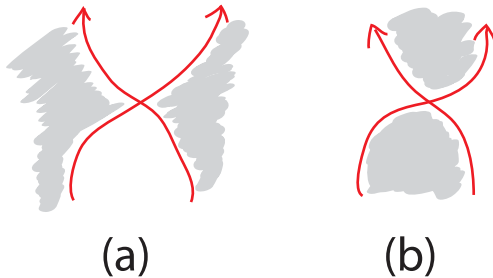


Figure 12: In admissible configuration of zig-zag paths we only have (a) as a possibility. However, if we lift admissibility condition, there are two possible types of intersections, and correspondingly we need two different weights. Red lines represents zig-zag paths, and gray region represents colored region.

How is this related to our index? First, let us specialize the BS model to the case with admissible zig-zag paths. Then the case (b) in Figure 12 does not arise. The claim is that in this case the Boltzmann weights of BS model coincides with that of the 4d index, up to a spin-independent (but rapidity-dependent) overall normalization of the partition function.

Let us see this explicitly for $N = 2$. In this case we can write $z_v = (z_v, z_v^{-1})$ and the weights are

$$I_{\text{chiral}}^e(z_{s(e)}, z_{t(e)}) = \Gamma((pq)^{1/2} z_{s(e)}^{\pm 1} z_{t(e)}^{\pm 1} u_{L(e)} u_{R(e)}^{-1}; p, q) , \quad (3.42)$$

where here we meant the product of four terms with plus/minus signs. We also have (see (A.2) and (A.7))¹⁰

$$I_{\text{vect}}^v(z) = (pq)^{-1/8} \theta_1\left(\frac{\sigma_v}{\pi} \middle| p^{1/2}\right) \theta_1\left(\frac{\sigma_v}{\pi} \middle| q^{1/2}\right) . \quad (3.43)$$

¹⁰Contrary to [11] we have included the factor $1/N!$ in the measure, not in I_{vect} .

These are identified with the weights function \mathcal{W}_α and \mathcal{S} of [11]¹¹, except by an overall spin-independent normalization factor for I_{chiral} .

The subtle difference in the normalization arises since statistical physicists and gauge theorists have different motivations. First, BS model requires a stronger invariance, *i.e.*, invariance under moves violating admissibility conditions (Figure 8), and the specific normalization was chosen to serve that purpose. This is not necessary for 4d index. Second, 4d index has a very specific normalization build into the definition, whereas as a statistical mechanical problem we can multiply I_{vector} by a constant depending on the chemical potentials p, q and u . For example, the two moves of Figure 6 preserves the number of the vertices of the quiver, and any overall multiplicative factor associated with the vertex hence preserves the invariance under the two moves. In fact, contrary to [11], we are not normalizing the values of the partition function in the thermodynamic limit.

As we explained in section 2.3, the reason we stick to the admissibility condition is that we do not have a known Lagrangian for brane configurations for general D5/NS5 brane configurations. The fact that we can extend the integrable spin system to non-admissible configuration could be suggesting that the Seiberg duality extends to theories on multiplet NS5-branes.

Comments

Several comments are now in order.

First, the statistical mechanical model here is invariant under the moves in Figure 8, and has Z-invariance [53, 54] (studied originally by Baxter in the context of eight-vertex models).

Second, in general the Boltzmann weight for the model is not real and positive [12], which might look problematic as a statistical mechanical model. However, in our context we are computing the index and the answer necessarily comes with negative contributions.

Third, note that the resulting spin model is in general chiral, except for the case $N = 2$, where there is no distinction between fundamental and anti-fundamental representation. This explains why the multi-component spin models of [12] requires the chirality (and therefore extra combinatorial data), as opposed to the $N = 2$ case of [11].

Fourth, in the integrable models there is a duality transformation exchanging the graph \mathcal{G} with its dual \mathcal{G}^* , which is a generalization of duality of the Using model exchanging high-temperature expansion with the low-temperature expansion. In our gauge

¹¹The parameters p, q here are denoted by p^2, q^2 in [11].

theory context this duality is broken; for example \mathcal{G}^* is a bipartite graph, but \mathcal{G} is not in general.

Fifth, in the analysis to this point we have concentrated on the 4d index on $S^1 \times S^3$. However, as is clear from the argument above the specific choice of this observable in itself does not matter — other quantities will serve the same purpose as long as (1) they are invariant under the Seiberg duality and integrating out massive matters (2) the quantity takes a factorized form as in (3.10).

As an example of such quantity, we could use the 4d lens space index computed in [29]. This is a index on $S^1 \times L(p, q)$, where $L(p, q)$, with p and q coprime integers, is the lens space (\mathbb{Z}_p orbifold of S^3). The complication for this case is that we have a set of integers, which parametrize the discrete Wilson line. This means that the corresponding spin chain has integer as well as continuous labels, and could not be interpreted as a conventional statistical mechanical model. This lens space index has a reduction to 3d superconformal index in the $p \rightarrow \infty$ limit [29], which suggests a generalization of the contents of the next section concerning 3d S^3 partition function to the 3d superconformal index.

Finally, let us make a brief comment on the comparison with the existing literature. The invariance of the index under the Seiberg duality for quiver gauge theories has been studied for some examples in [55]. The results of this section apply to more general quiver gauge theories dual to an arbitrary toric Calabi-Yau manifold. Note also the relation of the 4d index and the statistical mechanical model is known to experts, for example in [52]. However, to the best of my knowledge the correspondence with the supersymmetric quiver gauge theories has never been worked out in detail, and as we have seen there are in fact some subtle differences between the statistical mechanical models in the literature and the spin system defined from the 4d superconformal index. Moreover, as we will see in the next section we will see that this insight leads to a remarkable connection between 3d $\mathcal{N} = 2$ gauge theories and the geometry of 3d hyperbolic 3-manifolds.

4 Reduction to 3d and 2d

4.1 Reduction to 3d

The spin system defined in the previous section is based on a rather general solution of the Yang-Baxter-type equation, and several known integrable models, including the Kashiwara-Miwa model [56] and the chiral Potts model [57, 58, 59] (and their sl_N generalizations), arise as a specialization/limit of the solution. Therefore it is natural to ask

whether there are some natural limits which is of direct interest in the context of gauge theory.

In gauge theory there is one obvious limit. Since we have a 4d theory on $S^1 \times S^3$, we could dimensionally reduce along the S^1 . The resulting theory has 3d $\mathcal{N} = 2$ symmetry, and by flowing to the IR we obtain a new 3d SCFT. We always need to keep in mind that there is non-trivial RG flow involved in this process; in particular, the anomalous dimensions in 4d and in 3d are in general different. This reduction is also a natural in terms of integrable models — it is simply the high-temperature limit of the theory.

The effect of this S^1 reduction on the superconformal index has been studied in [60, 61, 46, 62], and we obtain a 3d partition function on ellipsoid S_b^3 [63] (generalizing the earlier results for $S_{b=1}^3$ [64, 65, 66])

$$S_b^3 = \{(z_1, z_2) \in \mathbb{C}^2 \mid b^2 |z_1|^2 + b^{-2} |z_2|^2 = 1\} . \quad (4.1)$$

To see this explicitly, first note that when the thermal S^1 shrinks all the chemical potentials p, q, u go to 1, but we could keep the ratio fixed and finite:¹²

$$p = e^{-\beta(1+\eta)}, \quad q = e^{-\beta(1-\eta)}, \quad u_i = e^{-\beta\mu_i} . \quad (4.3)$$

For a 1-loop determinant of the chiral multiplet we have (see (3.18))

$$I_{\text{chiral}}^e = \prod_{j,k} \prod_{m,n \geq 0} \frac{1 - e^{-\beta[-i(\sigma_{s(e),j} - \sigma_{t(e),k}) - (R_e - 1 + \mu_{L(e)} - \mu_{R(e)}) + (m + \frac{1}{2})(1+\eta) + (n + \frac{1}{2})(1-\eta)]}}{1 - e^{-\beta[i(\sigma_{s(e),j} - \sigma_{t(e),k}) + (R_e - 1 + \mu_{L(e)} - \mu_{R(e)}) + (m + \frac{1}{2})(1+\eta) + (n + \frac{1}{2})(1-\eta)]}} . \quad (4.4)$$

In the limit $\beta \rightarrow 0$ we regularize the expression $1 - e^{-\beta x}$ to be

$$[x]_\beta := \frac{1 - e^{-\beta x}}{1 - e^{-\beta}} \rightarrow x, \quad \text{as } \beta \rightarrow 0 , \quad (4.5)$$

and I_{chiral}^e reduce to Z_{chiral}^e , which is given by

$$\begin{aligned} Z_{\text{chiral}}^e &= \prod_{j,k=1}^N \prod_{m,n \geq 0} \frac{-i(\sigma_{s(e),j} - \sigma_{t(e),k}) - (r_e - 1) + (m + \frac{1}{2})(1 + \eta) + (n + \frac{1}{2})(1 - \eta)}{i(\sigma_{s(e),j} - \sigma_{t(e),k}) + (r_e - 1) + (m + \frac{1}{2})(1 + \eta) + (n + \frac{1}{2})(1 - \eta)} \\ &= \prod_{j,k=1}^N \prod_{m,n \geq 0} \frac{\frac{Q}{2} (-i(\sigma_{s(e),j} - \sigma_{t(e),k}) - (r_e - 1)) + (m + \frac{1}{2})b + (n + \frac{1}{2})b^{-1}}{\frac{Q}{2} (i(\sigma_{s(e),j} - \sigma_{t(e),k}) + (r_e - 1)) + (m + \frac{1}{2})b + (n + \frac{1}{2})b^{-1}} \\ &= \prod_{j,k=1}^N s_b \left(\hat{\sigma}_{s(e),j} - \hat{\sigma}_{t(e),k} + \frac{iQ}{2} (1 - r_e) \right) , \end{aligned} \quad (4.6)$$

¹² In t, y, u variables this is to take

$$t = e^{-\beta/3}, \quad \eta = e^{-\beta\eta}, \quad u_i = e^{-\beta\mu_i} , \quad (4.2)$$

which coincides with the limit taken in [61] for 4d $\mathcal{N} = 2$ theories.

where we defined

$$b = \sqrt{\frac{1+\eta}{1-\eta}}, \quad (4.7)$$

and $s_b(z)$, the quantum dilogarithm function defined in appendix, is used to regularize the infinite product (A.20). In the last line we re-defined σ by a factor of $\frac{Q}{2}$: $\hat{\sigma} := \frac{Q}{2}\sigma$.

We also defined the R-charge r_e by

$$r_e = R_e + \mu_{L(e)} - \mu_{R(e)}. \quad (4.8)$$

Here the parameters μ_i play the role of the real mass parameters obtained by weakly gauging the i -th global symmetry. The equation (4.8) shows that the real mass parameters has the effect of changing the anomalous dimension (cf. [67]). This is consistent with the Römelsberger's prescription explained in section 3.1.

Similar analysis shows (after we regularize the divergence coming from $\kappa(p, q)$)

$$\begin{aligned} I_{\text{vect}}^v \rightarrow Z_{\text{vect}}^v &= \prod_{i < j} s_b \left(\hat{\sigma}_{v,i} - \hat{\sigma}_{v,j} + \frac{iQ}{2} \right) s_b \left(-(\hat{\sigma}_{v,i} - \hat{\sigma}_{v,j}) + \frac{iQ}{2} \right), \\ &= \prod_{i < j} 4 \sinh b (\hat{\sigma}_{v,i} - \hat{\sigma}_{v,j}) \sinh b^{-1} (\hat{\sigma}_{v,i} - \hat{\sigma}_{v,j}). \end{aligned} \quad (4.9)$$

We will drop the overall multiplicative constant 4 in the following. Note that the invariance of the index under $y \leftrightarrow y^{-1}$ (3.2) is translated into the invariance $b \leftrightarrow b^{-1}$. The full partition is still written as a matrix integral of these 1-loop determinants

$$Z_{3d} = \int \left(\prod_{v \in V} d\sigma_v \right) \left(\prod_{v \in V} Z_{\text{vector}}^v \right) \left(\prod_{e \in E} Z_{\text{chiral}}^e \right), \quad (4.10)$$

which is precisely the 3d partition function on an ellipsoid. Note that in our story not all the real mass parameters of the theory are turned on. This is because we started from the 4d theory; some 3d global symmetries are anomalous in 4d and cannot be included in the 4d index.

Our 4d superconformal index has an invariance with respect to the two fundamental moves. Our 3d partition function to have the same property, since the latter is simply the limit of the former. For example, in the same notation as in (3.25), the effect of move I is represented by

$$\prod_{i,j} s_b \left(\hat{\sigma}_{v,i} - \hat{\sigma}_{v',j} + \frac{iQ}{2}(1 - r_e) \right) \prod_{i,j} s_b \left(\hat{\sigma}_{v',i} - \hat{\sigma}_{v,j} + \frac{iQ}{2}(1 - (2 - r_e)) \right). \quad (4.11)$$

This is trivial due to the relation (A.22). Of course, this is simply the limit of the relation (3.25).

4.2 Higgsing

To make contact with the geometry of hyperbolic 3-manifolds, we need to do one more reduction. For clarity let us specialize to the case $N = 2$ from here on.

As stated in the introduction, we give a VEV to the vector multiplet scalar for the diagonal gauge group $U(1)_{\text{diag}}$

$$U(1)_{\text{diag}} \subset SU(2)^{|V|} , \quad (4.12)$$

and send the VEV to infinity.

More concretely, let us write the vector multiplet scalar for the $U(1)_{\text{diag}}$ symmetry as $\hat{\sigma}$, and Higgs the $U(1)_{\text{diag}}$ gauge symmetry by sending σ to infinity:

$$\hat{\sigma}_v^{\text{old}} \rightarrow \hat{\sigma}_v^{\text{new}} + \hat{\sigma}, \quad \sum_{v \in V} \hat{\sigma}_v^{\text{new}} = 0, \quad \hat{\sigma} \rightarrow \infty . \quad (4.13)$$

In this limit, the vector multiplet 1-loop determinant diverges to a constant independent of $\hat{\sigma}_v$, and after regularization we have

$$Z_{\text{vector}}^v \rightarrow Z'_{\text{vector}} = 1 . \quad (4.14)$$

This is simply the 1-loop determinant for the Abelian gauge theory, which means that the gauge group after Higgsing is simply given by

$$\left[\prod_{v \in V} U(1)_v \right] / U(1)_{\text{diag}} . \quad (4.15)$$

For the chiral multiplet, the 1-loop determinant in (4.6) for $N = 2$ reads

$$Z_{\text{chiral}}^e = \frac{s_b \left(\hat{\sigma}_{s(e)} + \hat{\sigma}_{t(e)} + \frac{iQ}{2} r_e^* \right) s_b \left(\hat{\sigma}_{s(e)} - \hat{\sigma}_{t(e)} + \frac{iQ}{2} r_e^* \right)}{s_b \left(\hat{\sigma}_{s(e)} + \hat{\sigma}_{t(e)} - \frac{iQ}{2} r_e^* \right) s_b \left(\hat{\sigma}_{s(e)} - \hat{\sigma}_{t(e)} - \frac{iQ}{2} r_e^* \right)} , \quad (4.16)$$

where we defined

$$r_e^* = 1 - r_e . \quad (4.17)$$

In the limit (4.13), two out of the four factors stays the same

$$s_b \left(\pm \left(\hat{\sigma}_{s(e)} - \hat{\sigma}_{t(e)} \right) + \frac{iQ}{2} r_e^* \right) \rightarrow s_b \left(\pm \left(\hat{\sigma}_{s(e)} - \hat{\sigma}_{t(e)} \right) + \frac{iQ}{2} r_e^* \right) , \quad (4.18)$$

whereas the other two factors behave¹³

$$s_b \left(\pm(\hat{\sigma}_{s(e)} + \hat{\sigma}_{t(e)}) + \frac{iQ}{2} r_e^* \right) \rightarrow e^{\pm \frac{i\pi}{2} (\pm(2\sigma + \hat{\sigma}_{s(e)} + \hat{\sigma}_{t(e)}) + \frac{iQ}{2} r_e^*)^2} . \quad (4.19)$$

After subtracting the divergences, most of the finite part cancels due to the \pm sign, and the only remaining term is

$$e^{-\frac{\pi Q}{2} (\hat{\sigma}_{s(e)} + \hat{\sigma}_{t(e)}) r_e^*} .$$

However, this cancels out when we sum over $e \in E$, because

$$\sum_{e \in E} (\hat{\sigma}_{s(e)} + \hat{\sigma}_{t(e)}) r_e^* = \sum_{v \in E} \hat{\sigma}_v \sum_{e: \text{around } v} r_e^* = 0 .$$

where we used (4.13) and that (thanks to (2.18))

$$\sum_{e: \text{around } v} r_e^* = 2 . \quad (4.20)$$

The chiral multiplet 1-loop determinant therefore becomes

$$Z_{\text{chiral}} \rightarrow Z'_{\text{chiral}} = \frac{s_b \left(\sigma_{s(e)} - \sigma_{t(e)} + \frac{iQ}{2} r_e^* \right)}{s_b \left(\sigma_{s(e)} - \sigma_{t(e)} - \frac{iQ}{2} r_e^* \right)} . \quad (4.21)$$

The total partition function still takes the form (4.10), except that the 1-loop determinants are replaced by $Z'_{\text{vector}}, Z'_{\text{chiral}}$. Using (see (A.17))

$$\frac{s_b \left(s + \frac{iQ}{2} r \right)}{s_b \left(s - \frac{iQ}{2} r \right)} = e^{Q s \pi r} \frac{e_b \left(s + \frac{iQ}{2} r \right)}{e_b \left(s - \frac{iQ}{2} r \right)} , \quad (4.22)$$

we see that this coincides with the Boltzmann weight $W_\theta(s)$ of the Faddeev-Volkov model [13, 14, 15] in [17] under the parameter identification between their rapidity θ_e^* ¹⁴ and the R-charge r_e^* (recall (2.14))

$$\theta_e^* = \pi r_e^* , \quad \theta_e := \pi - \theta_e^* = \pi r_e , \quad (4.23)$$

up to an overall normalization¹⁵. Again, the overall normalization worked out in [17] is not necessary for our purpose. This two-step reduction from the solution of the star-triangle relation in [11] to the Faddeev-Volkov model has been explained in a different manner in [52].

¹³The appearance of the exponential of the quadratic term represents the parity anomaly. This cancels out in our final expression.

¹⁴This is denoted by θ_e in [17].

¹⁵Our function e_b is denoted by φ in [17].

The Faddeev-Volkov model realizes Virasoro algebra on the lattice, see also the subsequent formulation of the discrete Liouville theory [68]. As explained in [18], Liouville theory could be thought of as a boundary theory of $SL(2, \mathbb{R})$ Chern-Simons theory, and plays crucial roles in the relation with 3d $\mathcal{N} = 2$ gauge theories. This suggests a more direct relation between the 2d spin system and the 3d hyperbolic geometry. In the story of [18] the geometric picture simplifies in the semi-classical limit of the Chern-Simons theory [20]. On the gauge theory side this limit is translated into the limit $b \rightarrow 0$, where S_b^3 in (4.1) degenerates to $\mathbb{R}^2 \times S_b^1$ (the radius of S_b^1 is small, and is given by b). In the following we are going to take exactly the same limit. It is worth pointing out that the same limit of the Faddeev-Volkov model has been analyzed in the seminal paper [17], which also studied the connection with circle patterns.

4.3 Further Reduction to 2d

Let us dimensionally reduce our theory further to 2d, by taking the $b \rightarrow 0$ limit of the S_b^3 partition function. The resulting theory has 2d $\mathcal{N} = (2, 2)$ supersymmetry. After the dimensional reduction 2d the vector multiplet scalar σ is complexified due to the Wilson lines along S_b^1 , and a 3d real mass parameter reduces to a twisted mass in 2d.

In this limit, quantum dilogarithms reduce to classical dilogarithms (A.24), and we have

$$Z'_{3d} \rightarrow Z_{2d} = \int d\sigma \exp \left[-\frac{1}{\pi b^2} \mathcal{W}_{2d}(\sigma) \right], \quad (4.24)$$

where the effective twisted superpotential \mathcal{W}_{2d} is given by

$$\mathcal{W}_{2d}(\sigma) = \mathcal{W}_{2d}(\rho) = -\frac{1}{2} \sum_{e \in E} \left[\tilde{l}(\rho_{s(e)} - \rho_{t(e)} + i\theta_e^*) - \tilde{l}(\rho_{s(e)} - \rho_{t(e)} - i\theta_e^*) \right]. \quad (4.25)$$

We have scaled the variable σ by $2\pi b$ (this comes the radius of S_b^1 as in the standard dimensional reduction)

$$\rho_e = 2\pi b \hat{\sigma}_e = \pi Q b \sigma_e, \quad (4.26)$$

and $\tilde{l}(x)$ is defined in (A.25) in Appendix. Because $\tilde{l}(x + 2\pi i) = \tilde{l}(x)$, we can regard θ_e as defined modulo $2\pi\mathbb{Z}$. This is consistent with the discussion in section 2.4. Note also the appearance of the classical dilogarithm represents the sum over the contributions of the KK modes along S_b^1 [69]¹⁶.

¹⁶There is a side remark about the integrable structure. In references [69, 70], the saddle point

The classical vacuum of this theory is determined from the saddle point equation of the twisted superpotential

$$\exp\left(\frac{\partial\mathcal{W}_{2d}}{\partial\rho_v}\right) = 1. \quad (4.27)$$

In our case, this is given by the ‘‘cross ratio equation’’ (which are closely related with the Hirota difference equations)

$$1 = \prod_{e \in E, s(e)=v} \frac{\cosh(\rho_{s(e)} - \rho_{t(e)} + i\theta_e^*)}{\cosh(\rho_{s(e)} - \rho_{t(e)} - i\theta_e^*)} \prod_{e \in E, t(e)=v} \frac{\cosh(\rho_{s(e)} - \rho_{t(e)} - i\theta_e^*)}{\cosh(\rho_{s(e)} - \rho_{t(e)} + i\theta_e^*)}. \quad (4.28)$$

4.4 Circle Patterns and Tetrahedra

Surprisingly, the effective twisted superpotential (4.25) as well as the saddle point equation (4.28) has a beautiful geometrical reformulation. For this purpose we need to add extra degrees of freedom to the bipartite graph. In most of our discussion in previous sections, the bipartite graph only contains combinatorial data — we do not need to specify the length of the edges (the only exception is the part where we discuss isoradial condition)¹⁷. Henceforth we parametrize the length and angles of the bipartite graph and zig-zag paths in the following manner.

Let us assign a parameter ρ_v at each vertex $v \in V$, and draw a circle with radius $r_v := e^{\rho_v}$ centered at v . The quantity ρ_v will be identified with the vector multiplet scalar (4.26) momentarily, and hence we use the same symbol. We moreover impose the condition that when v and v' are adjacent at an edge e the two circles intersect at an angle θ_e^* . This angle will again be identified θ_e^* introduced previously in (4.23). Let $\varphi_{v,e}$ to be an angle around vertex v (Figure 13), and elementary trigonometry shows that

$$e^{i\varphi_{v,e}} = \frac{e^{\rho_v} + e^{\rho_{v'} + i\theta_e^*}}{e^{\rho_v} + e^{\rho_{v'} - i\theta_e^*}} = e^{i\theta_e^*} \frac{\cosh(\rho_v - \rho_{v'} + i\theta_e^*)}{\cosh(\rho_v - \rho_{v'} - i\theta_e^*)}, \quad (4.29)$$

equation of effective twisted superpotential of a 2d theory is identified with the Bethe Ansatz equation of an associated integrable model. It is interesting to imagine if this integrable structure (which in turn is conjectured to be equivalent to the integrable structure of the dimer model [26]) could be related to the integrable structure of the spin system mentioned above. However, it should be kept in mind that at least the two should not simply be identified directly; the two spin systems are rather different. Another difference is that the rapidities in our spin system are the chemical potentials for our 4d index, whereas those in the context of [69, 70] are identified with the vector multiplet scalars.

¹⁷In the context of brane configurations studied in section 2.3 these quantitative datum do matter. For example, the area of the region of the $(N, 0)$ -brane represents the inverse square of the gauge coupling constant. However, the author is not aware of direct brane interpretation of the geometric construction presented in this section.

see Figure 13. We also have

$$\varphi_{v,e} + \varphi_{v',e} = 2\theta_e^* . \quad (4.30)$$

Note that the right hand side of this equation takes the same form as the expression in (4.28). Thus the cross-ratio equation is the statement that the angles around v sum up to 2π

$$\sum_{e: \text{around } v} \varphi_{v,e} = 2\pi , \quad (4.31)$$

where we used (see (4.20) and (4.23))

$$\sum_{e: \text{around } v} \theta_e^* \equiv 0 \pmod{2\pi\mathbb{Z}} . \quad (4.32)$$

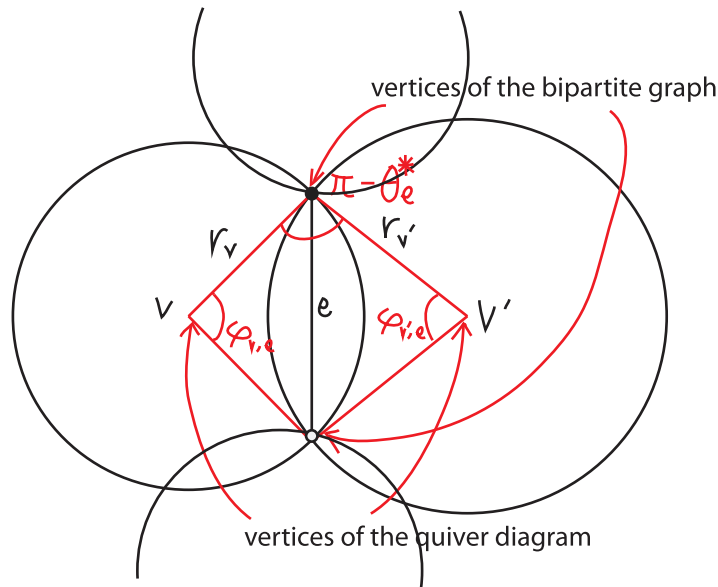


Figure 13: The two circles of radius r_v and $r_{v'}$, each centered at vertex v and v' connected with an edge e , intersect at an angle θ_e^* . This determines the angles $\varphi_{v,e}, \varphi_{v',e}$. The red quadrilateral is sometimes called a kite, and is a rhombus for an isoradial circle pattern.

Summarizing, the saddle point equation (4.28) is reformulated as a geometric condition on a set of circles intersecting at the vertices of the bipartite graph. In the literature a set of such circles is called a circle pattern¹⁸, and the deformation of a circle pattern represents the discrete analog of conformal transformation.

¹⁸In the case that $\theta_e^* = \frac{\pi}{2}$ for all $e \in E$, a circle pattern reduces to a circle packing together with its dual.

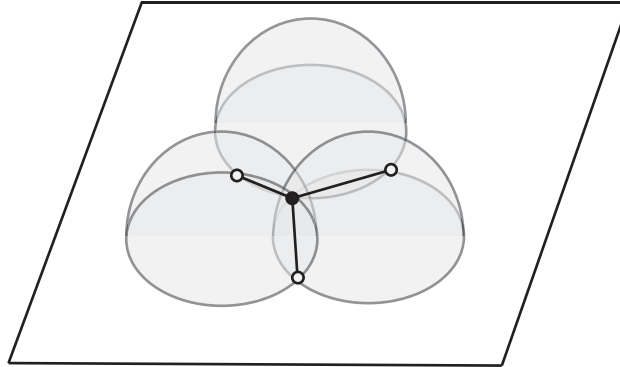


Figure 14: Our polyhedron M is defined as a complement of all the hemispheres.

For us, the importance of this geometric reformulation is that it gives the 3-manifold we are after¹⁹. To explain this, let us regard T^2 as part of the boundary \mathbb{R}^2 of \mathbb{H}^3 , and for each circle consider a hemisphere centered at v and intersecting the boundary \mathbb{R}^2 with the circle around v . Let us denote the region above all the hemispheres by M (Figure 14). Note that we still keep the torus identification on the boundary.

This could be equivalently described as follows. For each face $v \in F^* = V$ of the bipartite graph \mathcal{G}^* you can associate an ideal polyhedron Δ_v whose vertices are the vertices of \mathcal{G}^* at the face and at infinity. Then the polygon is defined as the union of all these ideal polyhedra, with neighboring faces glued together:

$$M = \bigcup_{v \in V} \Delta_v . \quad (4.33)$$

This is a hyperbolic 3-manifold (in the standard metric induced from that of \mathbb{H}^3), and has a geodesic boundary. In particular its hyperbolic volume is computed to be the sum of the volume of Δ_v , and depends non-trivially on ρ_v and θ_e^* .

The manifold M can be decomposed into hexahedra (Figure 15), which in turn could be divided into two non-ideal tetrahedra. As is clear from this definition, the gluing condition of the hexahedra at the vertices of the quiver diagram is exactly the condition (4.31), ensuring that the total angle around an edge of the polyhedron is 2π . We have therefore shown that the vacuum equations of the 2d gauge theory coincides with the gluing conditions of the 3-manifold M . As discussed in [1], the existence of the solution of the gluing condition is guaranteed by the 4d conditions on the R-charge (2.15), (2.17) and the result of [16].

¹⁹Historically the fact that a circle pattern has to do with the geometry of 3-manifolds is known since long ago, see for example [71, Chapter 13].

We can also directly compare the value of the twisted superpotential with the volume of the hyperbolic 3-manifold. We show that

$$\mathcal{W}_{2d}(\sigma)|_{\text{vacuum}} - \mathcal{W}_{2d}|_{\sigma=0} = \text{Vol}[M](\sigma)|_{\text{gluing}} - \text{Vol}[M_0] , \quad (4.34)$$

where the quantity $\text{Vol}[M_0]$, to be defined below, is independent of ρ_v , and we have evaluated the both sides at the values of ρ_v determined from the vacuum equations or gluing conditions. To evaluate the volume, we use the decomposition of M into hexahedra (Figure 15). The volume of the hexahedron at an edge e is given by [72, Lemma 4.2]

$$V_{\text{hexahedron}}^e = \mathcal{I}\left(\frac{\varphi_{s(e),e}}{2}\right) + \mathcal{I}\left(\frac{\varphi_{t(e),e}}{2}\right) \quad (4.35)$$

$$\begin{aligned} &= 2 \mathcal{I}\left(\frac{\theta_e^*}{2}\right) - \frac{1}{2} \left[\tilde{l}(\rho_{s(e)} - \rho_{t(e)} + i\theta_e^*) - \tilde{l}(i\theta_e^*) \right] \\ &\quad + \frac{1}{2} \left[\tilde{l}(\rho_{s(e)} - \rho_{t(e)} - i\theta_e^*) - \tilde{l}(-i\theta_e^*) \right] \\ &\quad + \frac{1}{4} (\varphi_{s(e),e} - \varphi_{t(e),e}) (\rho_{s(e)} - \rho_{t(e)}) , \end{aligned} \quad (4.36)$$

where in the last line we used (A.14), (A.27) in Appendix. The total volume of M is then given by summing over the edge e :

$$\text{Vol}[M]|_{\text{gluing}} = \sum_{e \in E} V_{\text{hexahedron}}^e|_{\text{gluing}} = \mathcal{W}_{2d}|_{\text{gluing}} - \mathcal{W}_{2d}|_{\sigma=0} + \text{Vol}[M_0] , \quad (4.37)$$

where we used that fact that the last term in (4.36) cancels out at the saddle point (see (4.13), (4.31), (4.32)), and we defined

$$\text{Vol}[M_0] := \sum_e 2 \mathcal{I}\left(\frac{\theta_e^*}{2}\right) . \quad (4.38)$$

As we will see shortly this is the value of $\text{Vol}[M]$ when the circle pattern is isoradial. This proves (4.34).

Isoradiality

In general, it is a difficult problem to analytically solve the cross ratio equations (4.28). Considerable simplification occurs when the graph is isoradial. Isoradial condition (section 2.2) states that it is geometrically possible to choose ρ_v such that

$$\rho_v = \rho \quad \text{independent of } v . \quad (4.39)$$

This is particularly useful for us because in this case (4.29) simplifies to

$$\varphi_e \equiv \theta_e^* \pmod{2\pi\mathbb{Z}} , \quad (4.40)$$

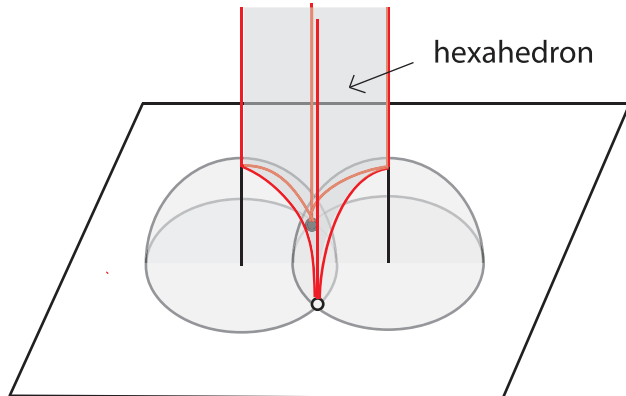


Figure 15: Our polygon M could be decomposed into hexahedra, each of which is associated with an edge of the bipartite graph. The projection of this hexahedron gives the red quadrilateral in Figure 13.

which automatically solves (4.31) (see (4.32)). There is an enhanced $SU(|V|)$ global symmetry at this vacuum.

In this vacuum the volume of M reduces to (4.38), and the critical value of the twisted superpotential vanishes,

$$\mathcal{W}_{2d}(\sigma)\Big|_{\text{isoradial}} = 0 . \quad (4.41)$$

Note that the isoradiality is not preserved under the two fundamental moves of Figure 6. However, the critical value of the twisted superpotential is still preserved under the fundamental moves.

Hyperbolic Circle Patterns

To this point we started with a geometric realization of the dimensionally reduced theory after the Higgsing. This raises a natural question: what if we start with the 3d theory before Higgsing and dimensionally reduce to 2d? Does this theory has geometric reformulation? The answer to the latter question is affirmative. Let us explain this briefly.

Let us go back to the expression of the partition function in section 4.1, and again let us take $N = 2$, in which case the chiral multiplet 1-loop determinant is given in (4.16). After the dimensional reduction as in section 4.3 (but without going through the Higgsing in section 4.2), the 2d vacuum equation is written as

$$\sum_{e: \text{ around } v} \tilde{\varphi}_{v,e} = 2\pi, \quad (4.42)$$

where $\tilde{\varphi}_{v,e}$ is defined by

$$e^{2i\tilde{\varphi}_{v,e}} = \frac{1 + e^{\rho_{v',e} - \rho_{v,e} + i\theta_e}}{1 + e^{\rho_{v',e} - \rho_{v,e} - i\theta_e}} \frac{1 + e^{\rho_{v',e} + \rho_{v,e} - i\theta_e}}{1 + e^{\rho_{v',e} + \rho_{v,e} + i\theta_e}}, \quad (4.43)$$

where the edge e connects the vertex v with another v' . The equation (4.43) is a trigonometric relation for the angle placed on Figure 13, but now placed on a *hyperbolic* plane \mathbb{H}^2 instead of \mathbb{R}^2 [72]. From this viewpoint the Higgsing in section 4.2 is a process of replacing circle patterns in \mathbb{H}^2 by those in \mathbb{R}^2 .

4.5 Comments on the Geometry of the 3-manifold

In the previous subsection our 3-manifold is obtained by gluing ideal polyhedra. Here are preliminary remarks on the geometry of this 3-manifold; more details are currently under investigation.

M5-brane Realizations

Let us comment on the brane realization of our 3d $\mathcal{N} = 2$ theory. We begin with the brane configuration in section 2.3, and in order to dimensionally reduce the theory to 3d we compactify and T-dualize along the 3-direction. Then we have a D4/NS5 system in type IIA:

		0	1	2	3	4	5	6	7	8	9	
N D4		-	-	-			·		·			
1 NS5		-	-	-	-		Σ					

(4.44)

This can be lifted to M-theory by including an extra 11-th direction:

		0	1	2	3	4	5	6	7	8	9	11	
N M5		-	-	-			·		·			-	
M5		-	-	-	-		Σ						

(4.45)

The resulting system is the intersection of two different types of M5-branes, where N M5-branes (coming from D5-branes in type IIB) wraps T^3 and another M5-brane (coming from the NS5-brane) wraps a special Lagrangian submanifold M' in $\mathbb{R}^3 \times T^3$. Note that M' and T^3 , two different types of M5-branes, intersect along a one dimensional subspace²⁰. This brane configuration tells us that M' is the Riemann surface fibered over the S^1 ; of course, this S^1 is part of the $S^1 \times S^3$ on which we compactified 4d gauge

²⁰Similar brane configuration has been studied in [73].

theory. This places a strong constraint on the geometry of M' . It is a future problem to clarify the precise relation between M' and our 3-manifold M .

M As a Link Complement

Our 3-manifold M is a link complement, at least in some special situations. Let us illustrate this with a simple example, following [74, Appendix] and [75].

Suppose that we start with a bipartite graph shown in Figure 16 (a). The corresponding Calabi-Yau geometry is the canonical bundle over $\mathbb{P}^1 \times \mathbb{P}^1$. Suppose that the R-charge of all the fields are $1/2$. The circle pattern then is a circle packing with its dual (Figure 16 (a), green circles). The bipartite graph \mathcal{G}^* have four faces (gauge groups), and we choose a checkerboard coloring of the faces²¹ (Figure 16 (b)). We first glue two colored faces. The resulting manifold has a boundary. We next prepare an identical copy of this partially glued polyhedron and then glue the two along the remaining uncolored faces. This gives a link complement, shown in Figure 16 (d).

More generally, this procedure works if (1) a circle pattern is given by a circle packing with its dual, *i.e.*, when the R-charges are all canonical, (2) the vertices of the quiver diagram can be checkerboard colored and (3) choose a particular pairing of the black faces. For example, this works for all the orbifolds of the example in Figure 16 with canonical R-charges.

5 Dimers and BPS State Counting

In this section we study the relations of our results to BPS state counting and topological string theory.

5.1 Thermodynamic Limit of Dimers

Let us first begin with the observation that the Legendre transform of the volume of the 3-manifold M when the circle pattern in isoradial coincides with the thermodynamic limit of a dimer partition function.

Suppose that I have a dimer model on T^2 . We choose a parametrization of the weight e^{ν_e} for an edge $e \in E$ by an angle (“rhombus angle”) θ_e^* :

$$e^{\nu_e} = 2 \sin \frac{\theta_e^*}{2} . \tag{5.1}$$

²¹This coloring is different from the coloring described in section 2.1.

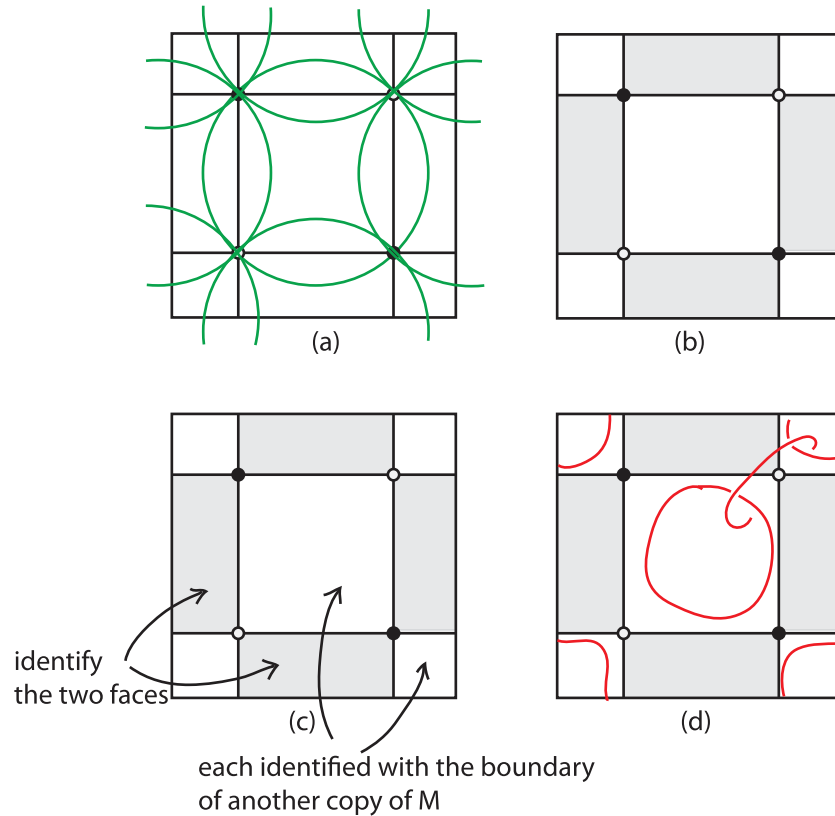


Figure 16: From two identical copies of our 3-manifold M we obtain the link complement shown in (d). We first start with a circle packing and its dual (a). We then choose a checkerboard coloring of the faces (b), and then pairwise glue the colored faces. This leaves a polyhedron with uncolored faces as boundaries, together with its copy. We finally glue the two polyhedra along the uncolored faces, and obtain a link complement in (d).

Note that this is the logarithm of the length of the edge e in Figure 13. The partition function of this dimer model is defined by

$$Z_1 = \sum_{m: \text{ perfect matching}} \prod_{e \in m} e^{\nu_e} , \quad (5.2)$$

where the sum is over perfect matchings, *i.e.*, subsets of edges of the bipartite graph containing each vertex once and exactly once.

Let us consider the thermodynamic limit of this partition function. As is standard in statistical mechanics, this limit is taken by enlarging the size of the torus by n times in the two directions of the torus. Let Z_n be the partition function of this model. In the large n limit, the free energy scales as n^2 , and we could extract a finite quantity by taking the scaling limit. In the case that the dimer is isoradial, this is computed to be [76, 77]²²

$$2\pi \lim_{n \rightarrow \infty} \frac{1}{n^2} \log Z_n = \sum_{e \in E} \left(\theta_e^* \log 2 \sin \frac{\theta_e^*}{2} + 2 \mathcal{J} \left(\frac{\theta_e^*}{2} \right) \right) =: \tilde{V}(\nu) . \quad (5.3)$$

This quantity is originally introduced as a normalized determinant of the discrete Dirac operator [76]. This is consistent with the fact that dimers are described by free fermions, and the dimer partition function is the determinant of the Dirac operator.

The expression (5.3) is not exactly the volume itself (4.38), but its Legendre transform. In fact, there is a general analysis of the thermodynamic limit of the dimer model in [78], which is applicable to arbitrary (not necessarily isoradial) dimers. There it has been shown that the Legendre transformation of the thermodynamic limit of the dimer partition function (the left hand side of (5.3)) is the Ronkin function R (explained in Appendix B) of the spectral curve of the dimer model, and is given by the Legendre transformation of the surface tension σ :

$$\tilde{V}(\nu) = \sum_{e \in E} \theta_e^* \nu_e + \sigma(\theta^*) , \quad (5.4)$$

where θ_e^* is the conjugate variable to ν_e . By definition θ_e^* can be computed as the probability of the edge e to be chosen in a perfect matching, and is shown to be related to θ_e^* by (5.1) [76].

This fact is powerful enough to determine $\sigma(\theta^*)$. In fact, from the property of the Legendre transformation we have

$$\frac{\partial \sigma(\theta^*)}{\partial \theta_e^*} = -\nu_e = -\log 2 \sin \frac{\theta_e^*}{2} , \quad (5.5)$$

²²Our θ_e^* here differs from θ in [76, 77] by a factor of 2.

and by integrating with respect to θ_e^* (see (A.9)) we obtain

$$\sigma(\theta^*) = \sum_{e \in E} 2 \mathcal{J} \left(\frac{\theta_e^*}{2} \right) = \text{Vol}[M_0] . \quad (5.6)$$

By combining (5.4) and (5.6) we obtain (5.3). In Appendix B we demonstrate (5.3) by an explicit computation for a simple example.

Summarizing, we have seen that the Legendre transform of the volume of the polygon M coincides with the thermodynamic limit of the dimer partition function.

Comments on F-extremization

Before proceeding to a next subsection there is a side remark on IR anomalous dimensions. The combination (5.3) can be rewritten as

$$\begin{aligned} \theta^* \log \left(2 \sin \frac{\theta^*}{2} \right) + 2 \mathcal{J} \left(\frac{\theta^*}{2} \right) \\ = -2\pi \left[-z \log(1 - e^{2\pi iz}) + \frac{i}{2} \left(\pi z^2 + \frac{1}{\pi} \text{Li}_2(e^{2\pi iz}) \right) - \frac{i\pi}{12} \right] , \end{aligned} \quad (5.7)$$

where $\theta^* = 2\pi z$ and the function inside the bracket is the function $l(z)$ defined in [65], which appears in the 1-loop determinant for the $S_{b=1}^3$ partition function. This means that the extremization of the dimer partition function coincides with the extremization of the integrand of the $S_{b=1}^3$ partition function in [65], and hence the IR anomalous dimension in the saddle point approximation of the matrix model²³. The author is not aware of an immediate application of this fact, nevertheless it would be interesting to explore if there is any further implication of this observation.

5.2 Relation with Topological Strings

We have seen that our partition function coincides with the thermodynamic limit of the dimer partition function. The same dimer partition function appears in the physics of BPS state counting and topological string theory (see [79, 80] for summary).

Let us consider type IIA string theory on the toric Calabi-Yau X_Δ . We consider BPS bound states of D0/D2-branes wrapping 0/2-cycles of X_Δ bound to a single D6-brane filling the whole X_Δ ²⁴. Equivalently these bound states are 1/2 BPS particles of the 4d $\mathcal{N} = 2$ supersymmetric gauge theory.

²³ A caveat in this statement is that there is a 3d global symmetry which is anomalous and not included in the superconformal index in 4d.

²⁴ We can define the crystal melting model with D4-branes wrapping 4-cycles included, however its thermodynamic limit has some additional subtlety due to the existence of the ‘‘gas phase’’ [78].

We define the BPS partition function as the generating function of the BPS degeneracies of these bound state of D-branes (mathematically this is the generating function for the generalized Donaldson-Thomas invariants):

$$Z_{\text{BPS}}(g_s, t) = \sum_{p_0, p_A} \Omega(p_0, p_A) e^{-g_{\text{top}} p_0 - t_A p_A} , \quad (5.8)$$

where p_0 and p_A are D0 and D2-brane charges, respectively, and Ω is the BPS degeneracy.

In the case the Calabi-Yau 3-fold is toric, then the BPS partition function is known to be described by the partition function of the crystal melting model, or equivalently a dimer model on \mathbb{R}^2 [81, 38, 82]. The resulting partition function takes an infinite product form, and is a reduction of a square of the topological string partition function [83]²⁵.

The thermodynamic limit of the dimer partition function in the previous subsection appears in the thermodynamic limit of this dimer model, *i.e.*, in the limit $g_{\text{top}} \rightarrow 0$. This limit has been analyzed in [78], and the limit (after suitable regularization) is an integral of the Ronkin function $R(x, y)$ of the spectral curve of the dimer model, which as shown in [31] coincides with the Riemann surface appearing in the mirror of the Calabi-Yau manifold (2.10). This leads to the identification

$$Z_{\text{BPS}} \rightarrow \exp \left[\frac{1}{g_s^2} \mathcal{F}_0 \right] , \quad \mathcal{F}_{\text{top}, 0} = \int dx dy R(x, y) , \quad (5.9)$$

where $\mathcal{F}_{\text{top}, 0}$ is the genus 0 prepotential of the topological B-model on the mirror \check{X}_Δ , or equivalently of the topological A-model on X_Δ , and the integral is over the amoeba defined in Appendix B. Combining these with our result (4.38) we see that an integral of the Legendre transform of the critical value of the effective twisted superpotential reproduces the genus 0 topological string partition function, as stated in (1.7).

$$\mathcal{F}_{\text{top}, 0} = \int dx dy \mathcal{L} \left[\text{Vol}[M] \Big|_{\text{isoradial}} \right] , \quad (5.10)$$

where \mathcal{L} represents the Legendre transformation described in section 5.1.

As a simple check of this relation, let us count the number of parameters. As we have seen, the twisted superpotential $\mathcal{W}_{2d}(\sigma)$, and therefore $\text{Vol}[M](\sigma)$, have $d - 1$ parameters. Because we integrate over two of them, we have $d - 3$ remaining parameters. This is the same as the number of compact P^1 in the geometry, and hence the number of Kähler moduli, for a toric Calabi-Yau 3-folds without compact 4-cycles.

²⁵Interestingly, this partition function could also be expressed as a matrix model [84, 85], which is again written in terms of dilogarithm functions and is similar to the matrix models considered in subsections 4.1 and 4.2. The spectral curve of this matrix model reproduces the mirror curve.

4d/1d correspondence

We have seen that a reduction of the 4d superconformal index for quiver gauge theories reproduces the topological string partition function on the dual geometry, the toric Calabi-Yau manifold. As we have explained above the two quantities are apparently of very different origin: one comes from 4d $\mathcal{N} = 1$ superconformal quiver *gauge theory* and another from the counting of BPS *particles* in toric Calabi-Yau. This raises the obvious question whether there is a natural explanation for this correspondence.

The simple answer is that the same bipartite graph (quiver and the superpotential) describes the two different physics, (1) 4d quiver gauge theory and (2) 1d quantum mechanics on the 1/2 BPS particles inside 4d $\mathcal{N} = 2$ theory²⁶. In this description, Seiberg duality in 4d mutates the quiver, which on the 1d side is interpreted as the crossing of the wall of marginal stability in the moduli space [86, 87]. Because the 4d index is invariant under Seiberg duality, we should recover a quantity which is not affected by wall crossing, and topological string partition function precisely satisfies this criterion.

This correspondence between 4d and 1d is strongly reminiscent of the correspondence [22] between the 3d $\mathcal{N} = 2$ gauge theories realized as domain walls in 4d $\mathcal{N} = 2$ theories and the 1/2 BPS particles in the same 4d $\mathcal{N} = 2$ theory, where the counterpart of a 4d Seiberg duality is played by a 3d mirror symmetry.

6 Concluding Remarks

We conclude with a few open problems, besides those already mentioned in introduction.

Our results, in particular the relation (1.1), are reminiscent of the recently found relation between 4d $\mathcal{N} = 2$ superconformal index and 2d TQFT [88, 89, 90]. There are many important differences between the two proposals; we have different class of 4d SCFTs (for example, our theories have Lagrangians whereas their theories do not in general) with different amount of supersymmetry ($\mathcal{N} = 1$ versus $\mathcal{N} = 2$). However, it is instructive to pursue the analogy between the two. For example, the counterpart of the decomposition of 4d $\mathcal{N} = 2$ SCFT from the pants decomposition of the Riemann surface [91] is the decomposition of the 4d $\mathcal{N} = 1$ SCFT from the partial resolution of the toric Calabi-Yau singularities, and the mirror of the resolution is indeed the pants decomposition of the mirror curve (2.8).

²⁶This was one of the key ingredients which lead to the construction of crystal melting model [82]. The subtle difference is that in (2) we have a D6-brane filling the whole X_Δ . This plays crucial roles in the wall crossing phenomena, but not for the consideration of this section.

The relation between the 2d spin system and the 3d $SL(2)$ Chern-Simons theory deserves further study. Since 3d $SL(2)$ Chern-Simons theory is closely related with 3d gravity, our 2d spin system could be regarded as a kind of spin network deconstructing 3d gravity.

In the discussion of 3-manifolds in this paper, the natural starting point was the 4d superconformal index. At the technical level this means that the quantum dilogarithm function arises as a limit of the elliptic gamma function. Since quantum dilogarithm function appears extensively in the geometry of 3-manifolds, wall crossing phenomena and 3d $\mathcal{N} = 2$ gauge theories²⁷, it is natural to ask if we could lift all these to the level of elliptic gamma functions. For example, is there a pentagon relation for elliptic gamma functions?

A somewhat related problem is to give a mathematical formulation of the superconformal index. Since our 4d theory is defined purely from the toric data there should be a mathematical formulation of the superconformal index in term of the geometry of the toric Calabi-Yau 3-fold, perhaps as an equivariant character of some moduli space²⁸. Pushing this further, there should be “categorified” versions of (1.1), (1.6), for example

$$\mathcal{H}_{4d \mathcal{N} = 1 \text{ SCFT on } S^3}^{\text{BPS}} = \mathcal{H}_{\text{moduli space defined from } X_\Delta} , \quad (6.1)$$

for some Hilbert space \mathcal{H} (similar categorified viewpoint has been advocated in [18]). Our results in section 5 suggest a relation of this Hilbert space with the moduli space of ideal sheaves on the Calabi-Yau manifold.

Acknowledgments

The author would like thank Yuji Terashima for collaboration on a companion paper [1] and for pointing out important references which are crucial for the completion of this work. He also thanks Tudor D. Dimofte, Leo P. Kadanoff, Sangmin Lee, Jessica S. Purcell, Salvatore Torquato, Grigory S. Vartanov, Dan Xie and Herman L. Verlinde for stimulating discussion and correspondence. He would like to thank the Bogoliubov

²⁷ The underlying mathematical structure is the cluster algebras, see [26] for relation with dimer models. The same mathematical structure appears recently in the study of scattering amplitudes [92], which also utilize zig-zag paths on bipartite graphs.

²⁸ This is related to the computation of the index on the gravity dual. However, our superconformal index does not capture the IR R-charge and hence should be formulated in the language of the toric Calabi-Yau cone, rather than of the Sasaki-Einstein manifold.

Laboratory of Theoretical Physics (JINR, Dubna), Newton Institute (Cambridge University) and Ludwig-Maximilians-Universität München for hospitality where part of this work has been performed. The results of this paper are presented at the conference “New perspectives on supersymmetric gauge theories” and the high energy theory seminar at Princeton University, and the author thanks the audience for feedback. Finally, he thanks Princeton Center for Theoretical Science for its generous support.

A Special Functions

In this appendix we summarize formulas for special function used in this paper.

We define the elliptic gamma function $\Gamma(z; p, q)$ by²⁹

$$\Gamma(z; p, q) = \prod_{j,k=0}^{\infty} \frac{1 - z^{-1}q^{j+1}p^{k+1}}{1 - zq^j p^k} . \quad (\text{A.1})$$

This is the basic building block for the 4d superconformal index. This function satisfies

$$\Gamma(z; p, q) = \frac{1}{\Gamma(pq/z; p, q)} , \quad (\text{A.2})$$

and

$$\Gamma(pz; p, q) = \theta(z; q)\Gamma(z; p, q), \quad \Gamma(qz; p, q) = \theta(z; p)\Gamma(z; p, q) , \quad (\text{A.3})$$

where $\theta(x; p)$ is the q -theta function defined by

$$\theta(z; q) = (z; q)_{\infty} (q/z; q)_{\infty} , \quad (\text{A.4})$$

with

$$(a; q)_{\infty} = \prod_{k=0}^{\infty} (1 - aq^k) . \quad (\text{A.5})$$

q -theta function is related to the Jacobi θ -function

$$\theta_1(z|q) = 2q^{1/4} \sin \pi z \prod_{m=1}^{\infty} (1 - q^{2m})(1 - 2 \cos 2\pi z q^{2m} + q^{4m}) , \quad (\text{A.6})$$

²⁹Beaware of the notational differences in comparison with the literature. For example, our notation here is different from that in [11].

by

$$\theta_1(z|q) = iq^{1/4}(q^2; q^2)_\infty e^{-\pi iz} \theta(e^{2\pi iz}; q^2) . \quad (\text{A.7})$$

The equation (A.3) is a elliptic generalization of the familiar relation $\Gamma(x+1) = x\Gamma(x)$. From (A.2), (A.3), (A.4) it follows that

$$\frac{1}{(1-z)(1-z^{-1})\Gamma(z; p, q)\Gamma(z^{-1}; p, q)} = \frac{1}{(1-z)^2} \theta(z; p)\theta(z; q) . \quad (\text{A.8})$$

As for the 3d and 2d partition functions, we need classical and quantum dilogarithms. The classical dilogarithm function (Euler dilogarithm) $\text{Li}_2(z)$ is defined by

$$\text{Li}_2(z) = - \int_0^z \frac{\log(1-t)}{t} dt = \sum_{n=1}^{\infty} \frac{z^n}{n^2} . \quad (\text{A.9})$$

A related function, Lobachevsky function $\mathcal{L}(x)$, is defined by

$$\mathcal{L}(x) = - \int_0^x dt \log |2 \sin t| . \quad (\text{A.10})$$

This could be expressed in terms of the Euler dilogarithm to be

$$2i \mathcal{L}(\theta) = \text{Li}_2(e^{2i\theta}) - \text{Li}_2(1) - \theta(\theta - \pi) , \quad (\text{A.11})$$

where the famous formula by Euler states that

$$\text{Li}_2(1) = \zeta(2) = \frac{\pi^2}{6} . \quad (\text{A.12})$$

By definition the Lobachevsky function is an odd function, $\mathcal{L}(-x) = -\mathcal{L}(x)$. Correspondingly, Euler dilogarithm satisfies

$$\text{Li}_2(-e^x) + \text{Li}_2(-e^{-x}) = -\frac{\pi^2}{6} - \frac{1}{2}x^2 , \quad (\text{A.13})$$

which is consistent with (A.12). We can also show

$$\mathcal{L}\left(\frac{\pi - \theta}{2}\right) = \mathcal{L}\left(\frac{\theta}{2}\right) - \frac{1}{2} \mathcal{L}(\theta) \quad (\text{A.14})$$

We also need the non-compact quantum dilogarithm functions $s_b(z)$ and $e_b(z)$ [14, 93, 94]. These functions are defined by

$$s_b(z) = \exp \left[\frac{1}{i} \int_0^\infty \frac{dw}{w} \left(\frac{\sin 2zw}{2 \sinh(bw) \sinh(w/b)} - \frac{z}{w} \right) \right] , \quad (\text{A.15})$$

and

$$e_b(z) = \exp \left(\frac{1}{4} \int_{-\infty+i0}^{\infty+i0} \frac{dw}{w} \frac{e^{-i2zw}}{\sinh(wb) \sinh(w/b)} \right), \quad (\text{A.16})$$

where the integration contour in (A.16) is chosen above the pole at $w = 0$. In both these expressions we require $|\text{Im } z| < |\text{Im } c_b|$ for convergence at infinity. There is a simple relation between the two functions

$$e_b(z) = e^{\frac{\pi iz^2}{2}} e^{-\frac{i\pi(2-Q^2)}{24}} s_b(z), \quad (\text{A.17})$$

and we loosely refer to both functions as quantum dilogarithms.

The function $s_b(z)$ satisfies a difference equation

$$s_b \left(z - \frac{ib^{\pm 1}}{2} \right) = 2 \cosh(\pi b^{\pm 1} z) s_b \left(z + \frac{ib^{\pm 1}}{2} \right), \quad (\text{A.18})$$

and hence

$$s_b \left(z - \frac{iQ}{2} \right) = 4 \sinh(\pi b^{-1} z) \sinh(\pi b z) s_b \left(z + \frac{iQ}{2} \right). \quad (\text{A.19})$$

We can use these equations to analytically continue $s_b(z), e_b(z)$ to the whole complex plane. The position of poles and the zeros are represented as

$$s_b(z) = \prod_{m,n \in \mathbb{Z}_{\geq 0}} \frac{mb + nb^{-1} + \frac{Q}{2} - iz}{mb + nb^{-1} + \frac{Q}{2} + iz}. \quad (\text{A.20})$$

where the left hand side is to be interpreted as a regularization of the right hand side. By definition we have

$$s_b(z) = s_{1/b}(z), \quad (\text{A.21})$$

and

$$s_b(z) s_b(-z) = 1. \quad (\text{A.22})$$

The asymptotic limit is given by

$$s_b(z) \rightarrow e^{\text{sgn}(z) \frac{i\pi z^2}{2}}, \quad \text{as } z \rightarrow \pm\infty. \quad (\text{A.23})$$

The name ‘‘quantum dilogarithm’’ could be justified by the fact that in the classical limit $b \rightarrow 0$, the quantum dilogarithm reduces to the classical dilogarithm:

$$e_b(z) \rightarrow \exp \left[\frac{1}{2\pi b^2} (-i) \text{Li}_2(-e^{2\pi b z}) \right], \quad s_b(z) \rightarrow \exp \left[\frac{1}{2\pi b^2} \tilde{l}(2\pi b z) \right], \quad (\text{A.24})$$

where

$$\begin{aligned}\tilde{l}(z) &:= (-i) \left[\text{Li}_2(-e^z) + \frac{1}{4}z^2 + \frac{\pi^2}{12} \right] = \frac{-i}{2} [\text{Li}_2(-e^z) - \text{Li}_2(-e^{-z})] \\ &= 2\mathfrak{I} \left(\frac{z}{2i} + \frac{\pi}{2} \right) .\end{aligned}\tag{A.25}$$

This function is odd, and its derivative is given by

$$\tilde{l}'(z) = i \log 2 \cosh \frac{z}{2} .\tag{A.26}$$

In the main text we need the following equality

$$\frac{1}{2} \left[\tilde{l}(\rho + i\theta) - \tilde{l}(\rho - i\theta) \right] = \mathfrak{I}(\theta) - \mathfrak{I} \left(\frac{\varphi_1}{2} \right) - \mathfrak{I} \left(\frac{\varphi_2}{2} \right) + \frac{1}{4}\rho(\varphi_2 - \varphi_1) ,\tag{A.27}$$

where φ_1, φ_2 are defined by

$$e^{i\varphi_1} = \frac{1 + e^{\rho+i\theta}}{1 + e^{\rho-i\theta}}, \quad e^{i\varphi_2} = \frac{1 + e^{-\rho+i\theta}}{1 + e^{-\rho-i\theta}}, \quad \varphi_1 + \varphi_2 = 2\theta .\tag{A.28}$$

The equality (A.27) can be proven with the help of the formula (this is a minor modification of [95, Proposition A])

$$\text{Li}_2(-e^{\rho+i\theta}) - \text{Li}_2(-e^{\rho-i\theta}) = 2i [\mathfrak{I}(\theta) - \mathfrak{I}(\omega) - \mathfrak{I}(\theta - \omega) - \omega\rho] ,\tag{A.29}$$

with

$$\tan \omega = \frac{e^\rho \sin \theta}{1 + e^\rho \cos \theta} \quad \text{i.e.,} \quad e^{2i\omega} = \frac{1 + e^{\rho+i\theta}}{1 + e^{\rho-i\theta}} .\tag{A.30}$$

B Hyperbolic Volume and Ronkin Function

In this appendix we first recall why the thermodynamic limit of the dimer partition function is given by the Ronkin function of the characteristic polynomial of the dimer model.

We then show in an explicit example that the Ronkin function is the Legendre transform of the hyperbolic volume of the polyhedron M . This equality is known in the literature, for example for \mathbb{C}^3 [96] and for a certain parametrization for the canonical bundle over $\mathbb{P}^1 \times \mathbb{P}^1$ [97].

Consider combinations of ν_e along closed non-trivial loops (α - and β -cycles) in T^2 , and let us denote them by e^x, e^y . These are the chemical potentials for the so-called

“height function” of the dimer model. Written in this variable, the partition function for the enlarged dimer Z_n (defined in section 5.1) is simply given by

$$Z_n(e^x, e^y) = \prod_{z^n=e^x} \prod_{w^n=e^y} Z_1(z', w') , \quad (\text{B.1})$$

where only the dependence of Z_n with respect to x, y are explicitly shown here. By taking a logarithm and dividing by n^2 , the product becomes a Riemann sum and we have

$$\lim_{n \rightarrow \infty} \frac{1}{n^2} \log Z_n(e^x, e^y) = \oint_{|z'|=|w'|=1} \frac{dz' dw'}{z' w'} \log |Z_1(e^x z', e^y w')| = R_{Z_1}(x, y) , \quad (\text{B.2})$$

where for a Laurent polynomial $P(z, w)$ we defined its Ronkin function R_P to be

$$R_P(x, y) = \frac{1}{(2\pi i)^2} \oint_{|z|=|w|=1} \frac{dz dw}{z w} \log |P(e^x z, e^y w)| . \quad (\text{B.3})$$

This is a convex function, and is linear outside the amoeba \mathcal{A}_P , defined by

$$\mathcal{A}_P = \{(x, y) \in \mathbb{R}^2 \mid \exists (\theta, \phi) \in (\mathbb{R}/2\pi\mathbb{Z})^2, P(e^{x+i\theta}, e^{y+i\phi}) = 0\} . \quad (\text{B.4})$$

In general it is not easy to work out the exact analytic expression for the Ronkin function. However, in many cases it is much simpler to compute its derivative by taking the residues of the integral.

Let us check the equality of (5.3) and (B.2) (times π) when Δ is the toric diagram for \mathbb{C}^3 . The dimer has three edges, whose weights we denote by x, y, z . Correspondingly we have three rhombus angles α, β, γ , which is related to x, y, z by

$$e^x = 2 \sin \alpha, \quad e^y = 2 \sin \beta, \quad e^z = 2 \sin \gamma .$$

and satisfying

$$\alpha + \beta + \gamma = \pi .$$

These weights satisfy the triangular inequality (we take $\alpha, \beta, \gamma \geq 0$)

$$e^x + e^y \geq e^z, \quad e^y + e^z \geq e^x, \quad e^z + e^x \geq e^y . \quad (\text{B.5})$$

The dimer partition function is

$$Z_1 = e^x + e^y + e^z , \quad (\text{B.6})$$

whose amoeba coincides with the region determined by (B.5). We now show

$$\pi R_{Z_1}(x, y, z) = \alpha x + \beta y + \gamma z + \mathcal{I}(\alpha) + \mathcal{I}(\beta) + \mathcal{I}(\gamma) . \quad (\text{B.7})$$

inside amoeba, where we defined the 3-variable version of Ronkin function by

$$R_P(x, y, z) = \frac{1}{(2\pi i)^3} \oint_{|u|=|v|=|w|=1} \frac{du}{u} \frac{dv}{v} \frac{dw}{w} \log |P(e^x u, e^y v, e^z w)|. \quad (\text{B.8})$$

This coincides with the 2-variable Ronkin function $R_{1+\frac{y}{x}+\frac{z}{x}}$ up to a constant factor.

To check (B.7) let us compute the derivative of the both sides of (B.7). The derivative of the left hand side inside amoeba can be evaluated by taking residues [98]

$$\pi \frac{\partial R_{Z_1}}{\partial x}(x, y, z) = \pi \frac{\partial R_{1+e^x+e^y}}{\partial x}(x-y, z-y) = \pi - \cos^{-1} \left(\frac{e^{2(x-y)} - e^{2(z-y)} - 1}{2e^{z-y}} \right) \quad (\text{B.9})$$

and hence by the law of cosines

$$\pi \frac{\partial R_{Z_1}}{\partial x} = \pi - \cos^{-1}(-\cos \alpha) = \alpha. \quad (\text{B.10})$$

The computation is similar for the y, z -derivatives, and the result coincides with the x, y, z -derivatives of the right hand side of (B.7). Note that the amoeba coincides with the region determined by (B.5).

References

- [1] Y. Terashima and M. Yamazaki, *Emergent 3-manifold from 4d Superconformal Index*, [arXiv:1203.5792](#). 3 pages, 2 figures.
- [2] A. Hanany and D. Vegh, *Quivers, tilings, branes and rhombi*, *JHEP* **0710** (2007) 029, [[hep-th/0511063](#)].
- [3] A. Hanany and K. D. Kennaway, *Dimer models and toric diagrams*, [hep-th/0503149](#).
- [4] S. Franco, A. Hanany, K. D. Kennaway, D. Vegh, and B. Wecht, *Brane dimers and quiver gauge theories*, *JHEP* **0601** (2006) 096, [[hep-th/0504110](#)].
- [5] S. Franco, A. Hanany, D. Martelli, J. Sparks, D. Vegh, *et. al.*, *Gauge theories from toric geometry and brane tilings*, *JHEP* **0601** (2006) 128, [[hep-th/0505211](#)].
- [6] K. D. Kennaway, *Brane Tilings*, *Int.J.Mod.Phys.* **A22** (2007) 2977–3038, [[arXiv:0706.1660](#)].
- [7] M. Yamazaki, *Brane Tilings and Their Applications*, *Fortsch.Phys.* **56** (2008) 555–686, [[arXiv:0803.4474](#)]. Master’s Thesis.

- [8] N. Seiberg, *Electric - magnetic duality in supersymmetric nonAbelian gauge theories*, *Nucl.Phys.* **B435** (1995) 129–146, [[hep-th/9411149](#)].
- [9] C. Romelsberger, *Counting chiral primaries in $N = 1$, $d=4$ superconformal field theories*, *Nucl.Phys.* **B747** (2006) 329–353, [[hep-th/0510060](#)].
- [10] J. Kinney, J. M. Maldacena, S. Minwalla, and S. Raju, *An Index for 4 Dimensional Super Conformal Theories*, *Commun. Math. Phys.* **275** (2007) 209–254, [[hep-th/0510251](#)].
- [11] V. V. Bazhanov and S. M. Sergeev, *A Master solution of the quantum Yang-Baxter equation and classical discrete integrable equations*, [arXiv:1006.0651](#).
- [12] V. V. Bazhanov and S. M. Sergeev, *Elliptic gamma-function and multi-spin solutions of the Yang-Baxter equation*, *Nucl.Phys.* **B856** (2012) 475–496, [[arXiv:1106.5874](#)].
- [13] A. Volkov, *Quantum Volterra model*, *Phys.Lett.* **A167** (1992) 345–355.
- [14] L. Faddeev and A. Y. Volkov, *Abelian current algebra and the Virasoro algebra on the lattice*, *Phys. Lett. B* **315** (1993), no. 3-4 311–318.
- [15] L. D. Faddeev, *Currentlike variables in massive and massless integrable models*, in *Quantum groups and their applications in physics (Varenna, 1994)*, vol. 127 of *Proc. Internat. School Phys. Enrico Fermi*, pp. 117–135. IOS, Amsterdam, 1996.
- [16] A. Bobenko and B. Springborn, *Variational principles for circle patterns and Koebe’s theorem*, [math/0203250](#).
- [17] V. V. Bazhanov, V. V. Mangazeev, and S. M. Sergeev, *Faddeev-Volkov solution of the Yang-Baxter equation and discrete conformal symmetry*, *Nucl.Phys.* **B784** (2007) 234–258, [[hep-th/0703041](#)].
- [18] Y. Terashima and M. Yamazaki, *$SL(2,R)$ Chern-Simons, Liouville, and Gauge Theory on Duality Walls*, [arXiv:1103.5748](#).
- [19] T. Dimofte and S. Gukov, *Chern-Simons Theory and S-duality*, [arXiv:1106.4550](#).
- [20] Y. Terashima and M. Yamazaki, *Semiclassical Analysis of the 3d/3d Relation*, [arXiv:1106.3066](#).

- [21] T. Dimofte, D. Gaiotto, and S. Gukov, *Gauge Theories Labelled by Three-Manifolds*, [arXiv:1108.4389](#).
- [22] S. Cecotti, C. Cordova, and C. Vafa, *Braids, Walls, and Mirrors*, [arXiv:1110.2115](#).
- [23] K. Nagao, Y. Terashima, and M. Yamazaki, *Hyperbolic 3-manifolds and Cluster Algebras*, [arXiv:1112.3106](#).
- [24] T. Dimofte, D. Gaiotto, and S. Gukov, *3-Manifolds and 3d Indices*, [arXiv:1112.5179](#).
- [25] T. Dimofte, S. Gukov, and L. Hollands, *Vortex Counting and Lagrangian 3-manifolds*, [arXiv:1006.0977](#).
- [26] A. Goncharov and R. Kenyon, *Dimers and cluster integrable systems*, [arXiv:1107.5588](#).
- [27] S. Franco, *Dimer Models, Integrable Systems and Quantum Teichmüller Space*, *JHEP* **1109** (2011) 057, [[arXiv:1105.1777](#)].
- [28] D. Xie, *Network, Cluster coordinates and $N=2$ theory I*, [arXiv:1203.4573](#).
- [29] F. Benini, T. Nishioka, and M. Yamazaki, *4d Index to 3d Index and 2d TQFT*, [arXiv:1109.0283](#).
- [30] L. F. Alday, D. Gaiotto, and Y. Tachikawa, *Liouville Correlation Functions from Four-dimensional Gauge Theories*, *Lett. Math. Phys.* **91** (2010) 167–197, [[arXiv:0906.3219](#)].
- [31] H. Ooguri and M. Yamazaki, *Emergent Calabi-Yau Geometry*, *Phys.Rev.Lett.* **102** (2009) 161601, [[arXiv:0902.3996](#)].
- [32] D. R. Gulotta, *Properly ordered dimers, R-charges, and an efficient inverse algorithm*, *JHEP* **0810** (2008) 014, [[arXiv:0807.3012](#)].
- [33] K. Ueda and M. Yamazaki, *A note on dimer models and McKay quivers*, *Commun.Math.Phys.* **301** (2011) 723–747, [[math/0605780](#)].
- [34] M. R. Douglas and G. W. Moore, *D-branes, quivers, and ALE instantons*, [hep-th/9603167](#).

- [35] I. R. Klebanov and E. Witten, *Superconformal field theory on three-branes at a Calabi-Yau singularity*, *Nucl.Phys.* **B536** (1998) 199–218, [[hep-th/9807080](#)].
- [36] R. Kenyon and J.-M. Schlenker, *Rhombic embeddings of planar quad-graphs*, *Trans. Amer. Math. Soc.* **357** (2005), no. 9 3443–3458 (electronic).
- [37] A. Ishii and K. Ueda, *A note on consistency conditions on dimer models*, in *Higher dimensional algebraic geometry*, RIMS Kôkyûroku Bessatsu, B24, pp. 143–164. Res. Inst. Math. Sci. (RIMS), Kyoto, 2011.
- [38] S. Mozgovoy and M. Reineke, *On the noncommutative Donaldson-Thomas invariants arising from brane tilings*, [arXiv:0809.0117](#).
- [39] Y. Imamura, *Global symmetries and 't Hooft anomalies in brane tilings*, *JHEP* **0612** (2006) 041, [[hep-th/0609163](#)].
- [40] Y. Imamura, H. Isono, K. Kimura, and M. Yamazaki, *Exactly marginal deformations of quiver gauge theories as seen from brane tilings*, *Prog. Theor. Phys.* **117** (2007) 923–955, [[hep-th/0702049](#)].
- [41] K. Hori, A. Iqbal, and C. Vafa, *D-branes and mirror symmetry*, [hep-th/0005247](#).
- [42] K. Hori and C. Vafa, *Mirror symmetry*, [hep-th/0002222](#).
- [43] B. Feng, Y.-H. He, K. D. Kennaway, and C. Vafa, *Dimer models from mirror symmetry and quivering amoebae*, *Adv.Theor.Math.Phys.* **12** (2008) 3, [[hep-th/0511287](#)].
- [44] A. Butti, *Deformations of Toric Singularities and Fractional Branes*, *JHEP* **0610** (2006) 080, [[hep-th/0603253](#)].
- [45] K. A. Intriligator and B. Wecht, *The Exact superconformal R symmetry maximizes a*, *Nucl.Phys.* **B667** (2003) 183–200, [[hep-th/0304128](#)].
- [46] Y. Imamura, *Relation between the 4d superconformal index and the S^3 partition function*, *JHEP* **1109** (2011) 133, [[arXiv:1104.4482](#)].
- [47] A. Kapustin and B. Willett, *Generalized Superconformal Index for Three Dimensional Field Theories*, [arXiv:1106.2484](#).

- [48] F. Dolan and H. Osborn, *Applications of the Superconformal Index for Protected Operators and q -Hypergeometric Identities to $N=1$ Dual Theories*, *Nucl.Phys.* **B818** (2009) 137–178, [[arXiv:0801.4947](#)].
- [49] E. M. Rains, *Transformations of elliptic hypergeometric integrals*, *Ann. of Math.* (2) **171** (2010), no. 1 169–243.
- [50] V. Spiridonov and G. Vartanov, *Elliptic Hypergeometry of Supersymmetric Dualities*, *Commun.Math.Phys.* **304** (2011) 797–874, [[arXiv:0910.5944](#)].
- [51] V. Spiridonov and G. Vartanov, *Elliptic hypergeometry of supersymmetric dualities II. Orthogonal groups, knots, and vortices*, [arXiv:1107.5788](#).
- [52] V. Spiridonov, *Elliptic beta integrals and solvable models of statistical mechanics*, [arXiv:1011.3798](#).
- [53] R. Baxter, *Solvable eight vertex model on an arbitrary planar lattice*, *Phil.Trans.Roy.Soc.Lond.* **289** (1978) 315–346.
- [54] R. Baxter, *Free-fermion, checkerboard and Z -invariant lattice models in statistical mechanics*, *Proc.Roy.Soc.Lond.* **A404** (1986) 1–33.
- [55] A. Gadde, L. Rastelli, S. S. Razamat, and W. Yan, *On the Superconformal Index of $N=1$ IR Fixed Points: A Holographic Check*, *JHEP* **1103** (2011) 041, [[arXiv:1011.5278](#)].
- [56] M. Kashiwara and T. Miwa, *A CLASS OF ELLIPTIC SOLUTIONS TO THE STAR TRIANGLE RELATION*, *Nucl.Phys.* **B275** (1986) 121.
- [57] R. Baxter, J. Perk, and H. Au-Yang, *New solutions of the star triangle relations for the chiral Potts model*, *Phys.Lett.* **A128** (1988) 138–142.
- [58] H. Au-Yang, B. M. McCoy, J. H. Perk, S. Tang, and M.-L. Yan, *Commuting transfer matrices in the chiral Potts models: Solutions of Star triangle equations with genus > 1* , *Phys.Lett.* **A123** (1987) 219–223.
- [59] G. von Gehlen and V. Rittenberg, *$Z(n)$ SYMMETRIC QUANTUM CHAINS WITH AN INFINITE SET OF CONSERVED CHARGES AND $Z(n)$ ZERO MODES*, *Nucl.Phys.* **B257** (1985) 351.

- [60] F. A. H. Dolan, V. P. Spiridonov, and G. S. Vartanov, *From 4D Superconformal Indices to 3D Partition Functions*, *Phys. Lett.* **B704** (2011) 234, [arXiv:1104.1787].
- [61] A. Gadde and W. Yan, *Reducing the 4d Index to the S^3 Partition Function*, arXiv:1104.2592.
- [62] T. Nishioka, Y. Tachikawa, and M. Yamazaki, *3d Partition Function as Overlap of Wavefunctions*, arXiv:1105.4390.
- [63] N. Hama, K. Hosomichi, and S. Lee, *SUSY Gauge Theories on Squashed Three-Spheres*, arXiv:1102.4716.
- [64] A. Kapustin, B. Willett, and I. Yaakov, *Exact Results for Wilson Loops in Superconformal Chern- Simons Theories with Matter*, *JHEP* **03** (2010) 089, [arXiv:0909.4559].
- [65] D. L. Jafferis, *The Exact Superconformal R-Symmetry Extremizes Z*, arXiv:1012.3210.
- [66] N. Hama, K. Hosomichi, and S. Lee, *Notes on SUSY Gauge Theories on Three-Sphere*, arXiv:1012.3512.
- [67] G. Festuccia and N. Seiberg, *Rigid Supersymmetric Theories in Curved Superspace*, *JHEP* **1106** (2011) 114, [arXiv:1105.0689].
- [68] L. D. Faddeev, R. M. Kashaev, and A. Y. Volkov, *Strongly coupled quantum discrete Liouville theory. I: Algebraic approach and duality*, *Commun. Math. Phys.* **219** (2001) 199–219, [hep-th/0006156].
- [69] N. A. Nekrasov and S. L. Shatashvili, *Supersymmetric vacua and Bethe ansatz*, *Nucl.Phys.Proc.Suppl.* **192-193** (2009) 91–112, [arXiv:0901.4744].
- [70] N. A. Nekrasov and S. L. Shatashvili, *Quantization of Integrable Systems and Four Dimensional Gauge Theories*, arXiv:0908.4052.
- [71] W. P. Thurston, *The geometry and topology of three-manifolds*, 1978-79.
- [72] B. Springborn, *Variational principles for circle patterns*, math/0312363.

- [73] S. Lee, *Superconformal field theories from crystal lattices*, *Phys.Rev.* **D75** (2007) 101901, [[hep-th/0610204](#)].
- [74] M. Lackenby, *The volume of hyperbolic alternating link complements*, *Proc. London Math. Soc. (3)* **88** (2004), no. 1 204–224. With an appendix by Ian Agol and Dylan Thurston.
- [75] J. S. Purcell, *An introduction to fully augmented links*, in *Interactions between hyperbolic geometry, quantum topology and number theory*, vol. 541 of *Contemp. Math.*, pp. 205–220. Amer. Math. Soc., Providence, RI, 2011.
- [76] R. Kenyon, *The Laplacian and Dirac operators on critical planar graphs*, *Invent. Math.* **150** (2002), no. 2 409–439.
- [77] B. de Tilière, *Partition function of periodic isoradial dimer models*, *Probab. Theory Related Fields* **138** (2007), no. 3-4 451–462.
- [78] R. Kenyon, A. Okounkov, and S. Sheffield, *Dimers and amoebae*, *Ann. of Math. (2)* **163** (2006), no. 3 1019–1056.
- [79] M. Yamazaki, *Crystal Melting and Wall Crossing Phenomena*, *Int.J.Mod.Phys.* **A26** (2011) 1097–1228, [[arXiv:1002.1709](#)].
- [80] P. Sulkowski, *BPS states, crystals and matrices*, *Adv. High Energy Phys.* **2011** (2011) 357016, [[arXiv:1106.4873](#)].
- [81] B. Szendroi, *Non-commutative Donaldson-Thomas theory and the conifold*, *Geom.Topol.* **12** (2008) 1171–1202, [[arXiv:0705.3419](#)].
- [82] H. Ooguri and M. Yamazaki, *Crystal Melting and Toric Calabi-Yau Manifolds*, *Commun.Math.Phys.* **292** (2009) 179–199, [[arXiv:0811.2801](#)].
- [83] M. Aganagic, H. Ooguri, C. Vafa, and M. Yamazaki, *Wall Crossing and M-theory*, *Publ.Res.Inst.Math.Sci.Kyoto* **47** (2011) 569, [[arXiv:0908.1194](#)].
- [84] H. Ooguri, P. Sulkowski, and M. Yamazaki, *Wall Crossing As Seen By Matrix Models*, *Commun.Math.Phys.* **307** (2011) 429–462, [[arXiv:1005.1293](#)].
- [85] R. J. Szabo and M. Tierz, *Matrix models and stochastic growth in Donaldson-Thomas theory*, [arXiv:1005.5643](#).

- [86] W.-y. Chuang and D. L. Jafferis, *Wall Crossing of BPS States on the Conifold from Seiberg Duality and Pyramid Partitions*, *Commun.Math.Phys.* **292** (2009) 285–301, [[arXiv:0810.5072](#)].
- [87] M. Aganagic and K. Schaeffer, *Wall Crossing, Quivers and Crystals*, [arXiv:1006.2113](#).
- [88] A. Gadde, E. Pomoni, L. Rastelli, and S. S. Razamat, *S-duality and 2d Topological QFT*, *JHEP* **1003** (2010) 032, [[arXiv:0910.2225](#)].
- [89] A. Gadde, L. Rastelli, S. S. Razamat, and W. Yan, *The 4d Superconformal Index from q-deformed 2d Yang-Mills*, [arXiv:1104.3850](#).
- [90] A. Gadde, L. Rastelli, S. S. Razamat, and W. Yan, *Gauge Theories and Macdonald Polynomials*, [arXiv:1110.3740](#).
- [91] D. Gaiotto, *N=2 dualities*, [arXiv:0904.2715](#).
- [92] N. Arkani-Hamed. Lecture at IAS, 2012.
- [93] L. D. Faddeev and R. M. Kashaev, *Quantum dilogarithm*, *Modern Phys. Lett. A* **9** (1994), no. 5 427–434.
- [94] L. D. Faddeev, *Discrete Heisenberg-Weyl group and modular group*, *Lett. Math. Phys.* **34** (1995), no. 3 249–254, [[hep-th/9504111](#)].
- [95] A. N. Kirillov, *Dilogarithm identities*, *Prog. Theor. Phys. Suppl.* **118** (1995) 61–142, [[hep-th/9408113](#)].
- [96] R. Cerf and R. Kenyon, *The low-temperature expansion of the Wulff crystal in the 3D Ising model*, *Comm. Math. Phys.* **222** (2001), no. 1 147–179.
- [97] H. Cohn, R. Kenyon, and J. Propp, *A variational principle for domino tilings*, *J. Amer. Math. Soc.* **14** (2001), no. 2 297–346 (electronic).
- [98] T. Fujimori, M. Nitta, K. Ohta, N. Sakai, and M. Yamazaki, *Intersecting Solitons, Amoeba and Tropical Geometry*, *Phys.Rev.* **D78** (2008) 105004, [[arXiv:0805.1194](#)].